

65563

**ELASTO-PLASTIC
STRESS ANALYSIS IN A COMPOSITE MATERIAL
WITH A SQUARE HOLE**

**A Thesis Submitted to the
Graduate School of Natural and Applied Science of
Dokuz Eylül University
In Partial Fulfillment of the Requirements for
the Master's Degree in Mechanical Engineering, Mechanics Program**

**by
Mehmet ŞENEL**

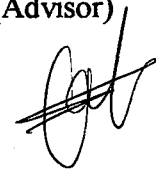
**January, 1997
İZMİR**

M. Sc. THESIS EXAMINATION RESULT FORM

We certify that we have read this thesis and that in our opinion it is fully adequate, in scope and in quality, as thesis for the degree of Master of Science.

Prof. Dr. Onur SAYMAN

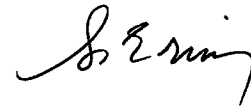
(Advisor)



Doc Dr. İsmail AKJOY
(Committee Member)

Doç. Dr. Sevil ERİN

(Committee Member)



Approved for the
Graduate School of Natural and Applied Sciences



Prof. Dr. Macit TOKSOY

Director

Graduate School of Natural and Applied Sciences

ACKNOWLEDGMENTS

I am deeply grateful to Prof. Dr. Onur SAYMAN for his patient supervision, valuable and continuous encouragement throughout this study.

I thank to Dr. Hamit AKBULUT for helping computer programming.

Mehmet ŞENEL



ABSTRACT

In this study, the elasto-plastic stress analysis of composite plates with a square hole has been obtained. Finite element method has been used to solve the problem. Isoparametric rectangular element with nine nodes has been chosen. The automatic mesh generation has been taken place in finite element model and the special computer program has been developed to solve the problem.

The engineering constants of composite material have been obtained by using strain gage in the tensile testing machine after production of the material (Stainless steel-aluminum composite) .

Finally, in this study, the distribution of the plastic region in the vicinity of the hole has been studied for different uniform loads, different hole diameter and different orientation angles. Furthermore, the plate is stronger because of resultant residual stresses.

ÖZET

Bu çalışmada ortasında kare delik bulunan kompozit bir plakta elasto-plastik gerilme analizi yapılmıştır. Problemin çözümünde sonlu eleman metodu kullanılmıştır. Eleman olarak dokuz düğümlü izoparametrik eleman seçilmiştir. Sonlu eleman modelindeki eleman ağı otomatik olarak elde edilmiş, problemin çözümü için özel bilgisayar programları kullanılmıştır.

Kompozit malzemeye ait mühendislik sabitleri, malzemenin (paslanmaz çelik-aluminyum kompoziti) üretiminden sonra çekme deneyi ile strain gage kullanılarak elde edilmiştir. Kompozit malzeme üretimi ekstrüzyon yolu ile üretilmiştir.

Sonuç olarak, bu çalışmada, plak üzerinde değişik uniform yayılı yükler, değişik delik çaplarında, değişik oryantasyon açılarında uygulanarak plastik bölgelerin delik çevresinde dağılımı incelenmiştir. Ayrıca oluşan artık gerilmelerle plağın mukavemeti artırılarak daha fazla yük taşıması sağlanmıştır.

CONTENTS

	Page
Contents.....	VI
List of Tables.....	IX
List of Figures.....	X

Chapter One

INTRODUCTION

1.1 Introduction.....	1
-----------------------	---

Chapter Two

THE FINITE ELEMENT METHOD

2.1 Introduction.....	2
2.2 Why The Finite Element Method.....	3
2.3 Finite Element Meshes.....	4
2.4 The Isoparametric Elements.....	5
2.5 Interpolation Function.....	6
2.5.1 Two Independent Variable.....	9
2.6 Interpolation Functions of Rectangular Elements.....	10
2.7 Natural Coordinates.....	10
2.8 Lagrange Polynomials.....	12
2.9 Obtaining The Element Properties.....	14

2.9.1 For The Isoparametric Finite Element Matrices.....	14
2.10 Obtaining The Element Properties.....	15
2.11 Calculation of Elasto-Plastic Stresses.....	18

Chapter Three

ANALYSIS OF COMPOSITE MATERIALS

3.1 Introduction.....	22
3.2 Properties of Composite Materials.....	22
3.2.1 Fibrous Composites.....	22
3.2.2 Properties of Matrices.....	23
3.3 Laminea.....	23
3.4 Laminates.....	25
3.5 Metal Matrix Composite Materials.....	26
3.6 Fabrication Methods for Metal Matrix Composites.....	26
Powder Metallurgy Technique.....	26
Liquid Metal Infiltration.....	27
Diffusion Bending.....	28
Electroforming.....	28
Vapor Deposition.....	29
Rolling.....	29
Extrusion.....	30
Other Methods.....	30
3.7 Properties of Aluminum-Stainless Steel Composites.....	31
3.7.1 Tensile Test in Elastic Region.....	31
3.7.2 Tensile Test in Elastic and Plastic Region	32
3.8 Stress-Strain Relations for Plane Stress in an Orthotropic Material.....	32
3.9 Experimental Determination of Strength and Stiffness.....	35
3.10 Biaxial Strength Theories For An Orthotropic Lamina.....	38
3.10.1 Maximum Stress Theory.....	38
3.10.2 Maximum Strain Theory.....	39

3.10.3 Tsai-Hill Theory.....	41
3.10.4 Tsai-Wu Tensor Theory.....	43
3.11 Elasto-Plastic Analysis of Orthotropic Materials.....	46

Chapter Four

DEFINITION AND FORMULATION

4.1 Definition of The Problem.....	47
4.2 Formulation of the Finite Element.....	48

Chapter Five

RESULTS AND CONCLUSION

5.1 Result and conclusion.....	49
--------------------------------	----



LIST OF TABLES

	Page
Table 3.1 Fiber and wire properties.....	2



LIST OF FIGURES

	Page
Figure 2. 1 Subdivided elements.....	3
Figure 2. 2 Two separate plane finite elements of unit uniform thickness.....	3
Figure 2. 3 Corners in two and three dimensions.....	5
Figure 2. 4 Automatic mesh generation by parabolic isoparametric elements.....	6
Figure 2. 5 Turbine blade modeled by solid elements.....	7
Figure 2. 6 Isoparametric elements.....	8
Figure 2. 7 Rectangular elements.....	9
Figure 2. 8 Cartesian and natural coordinates.....	11
Figure 2. 9 Interpolation using Lagrange Polynomials.....	13
Figure 2. 10 The rectangular isoparametric element.....	14
Figure 2. 11 Representation of initial stress method.....	20
Figure 3. 1 Two principal types of laminae.....	24
Figure 3. 2 Effect of broken fiber on matrix and fiber stresses.....	25
Figure 3. 3 Laminate Contraction.....	26
Figure 3. 4 Design of extrusion tooling.....	30
Figure 3. 5 Unidirectionally reinforced laminae.....	34
Figure 3. 6 Uniaxial loading in the 1-direction.....	36
Figure 3. 7 Uniaxial loading in the 2-direction.....	36
Figure 3. 8 Uniaxial loading at 45° to the 1-direction.....	37
Figure 3. 9 Cross-section of unidirectional lamina with fibers in the 1-direction.....	43
Figure 4. 1 Whole and square plate.....	49
Figure 4. 2 Mesh generation.....	50
Figure 5. 1 Plastic regions on quarter plates for $\theta=0^\circ$	52
Figure 5. 2 Plastic regions on quarter plates for $\theta=90^\circ$	53
Figure 5. 3 Plastic regions on whole plates for $\theta=30^\circ$	55
Figure 5. 4 Plastic regions on whole plates for $\theta=45^\circ$	57
Figure 5. 5 Plastic regions on whole plates for $\theta=60^\circ$	59
Figure 5. 6 A square plate for graphics.....	60

Figures 5. 7 Residual stresses on upper line of the hole for $\theta=0^0$	61
Figures 5. 8 Residual stresses on diagonal line for $\theta=0^0$	62
Figures 5. 9 Residual stresses on upper line of the hole for $\theta=90^0$	63
Figures 5. 10 Residual stresses on diagonal line for $\theta=90^0$	64
Figures 5. 11 A whole plate for graphics	64
Figures 5. 12 Residual stresses on upper line of the hole for $\theta=30^0$	65
Figures 5. 13 Residual stresses on upper line of the hole for $\theta=45^0$	66
Figures 5. 14 Residual stresses on upper line of the hole for $\theta=60^0$	67



CHAPTER ONE

INTRODUCTION

1. Introduction

With the increasing technology, it has been investigated to find new materials. When compared with other materials, composite materials have found a large usage area especially in plane, space and weapon industries. Nevertheless, the technology of metal-matrix composite materials is being developed very rapidly. The strength and elastic moduli of metal matrices are higher than those of resin matrices over a wide range of temperature. As to deformation of the composites, metal matrices can greatly enhance the ductility of the composite.

Karakuzu /2/, investigated increasing of strength of composite plates with semicircular holes under the elasto-plastic loads. Owen /4/, studied elasto-plastic finite element analysis of anisotropic plates and shell. Theo /6/, investigated stress around rectangular holes in orthotropic plates. Tsai /8/, searched finite element analysis of axisymmetric bodies under torsion. Zienkiewicz /9/, obtained two dimensional finite element analysis (plane stress, plane strain) of different isotropic structures.

In this study, the elasto-plastic stress analysis of the plates manufactured from steel-aluminum composite is made under the uniform tension loads. Distributions of plastic region near the notch and variations of residual stresses are investigated in the different orientation angles.

CHAPTER TWO

THE FINITE ELEMENT METHOD

2.1. Introduction

In this method the body is imagined to be actually broken up into a number of elements of finite dimension, hence its name. If the body has n ($=1,2,3$) dimensions of space, it is subdivided into a system of n -dimensional finite elements.

One-dimensional bodies will be subdivided into finite elements by means of nodes as in Figure 2. 1a; lines and planes will be used for the subdivision of two and three dimensional bodies, as shown in Figure 2. 1b and c respectively. In one-dimensional bodies the resulting finite elements may have unequal lengths, while in two and three dimensions they may have unequal sizes as well as unlike shapes. In all cases, however, the finite elements representing the body will be 'interconnected' by means of 'nodes' as shown in Figures 2. 1a, b and c. Thus, in the finite element method of analysis the body will be replaced by a system of finite elements and the nodes connecting them.

The precise manner in which finite elements are attached to the nodes is best understood by referring to Figure 2. 2; here we have two plane finite elements of unit uniform thickness, one triangular and other rectangular.

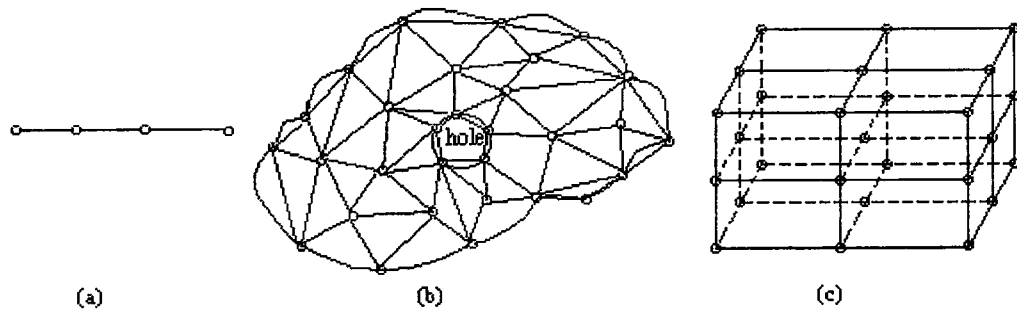


Figure 2. 1 (a) A one dimensional body subdivided into 3 linear elements.
 (b) A two dimensional body with a hole subdivided into a system of plane triangular elements. (c) Three dimensional body a b c d e f g h subdivided into 8 identical rectangular prism elements.

Clearly Figure 2. 2a, they are separate and not attached to each other in any way. we shall think of the nodes as ‘nut-and-bolt’ devices which secure adjacent finite elements through their ‘extremities’ and hold them together, as in Figure 2. 2b such that the elements will come apart when the nodes are removed. Clearly therefore, since they will come apart when the nodes securing them are removed. There is no physical continuity between adjacent finite elements.

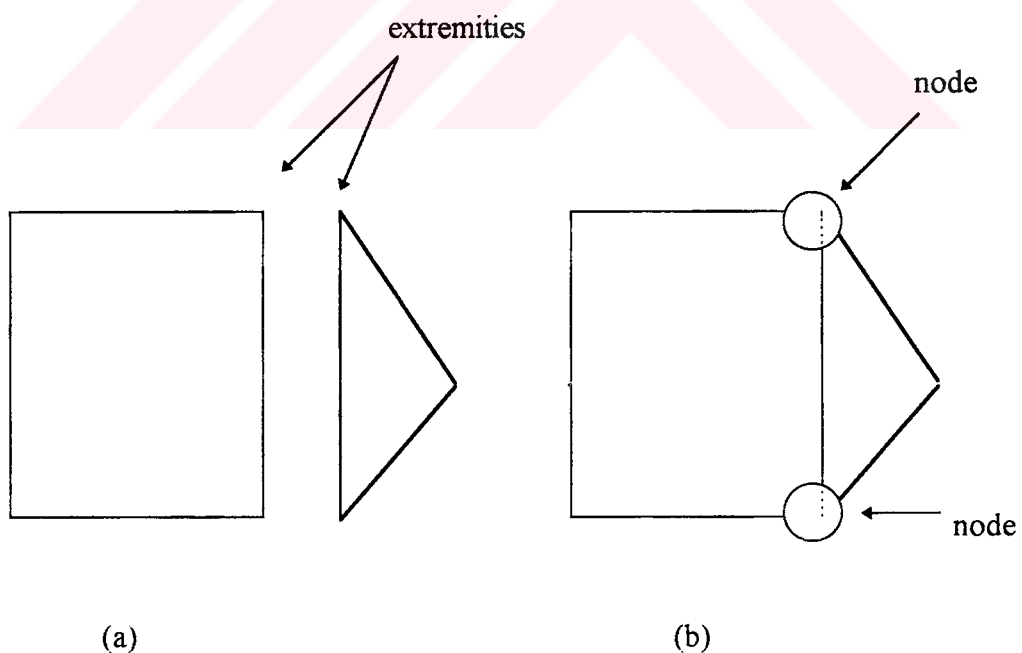


Figure 2. 2 (a) Two separate plane finite elements of unit uniform thickness.
 (b) The finites of (a) held together by means of nodes.

the next step in this method of analysis to determine the ‘element stiffness matrix’ of the individual elements representing the body. These will then be assembled to form the ‘overall stiffness matrix’ for the discretized (i.e. broken-up) body by requiring that the continuity of displacements and equilibrium of forces prevail at all nodes in the finite element model of the body. This will lead to the matrix equation

$$[K]\{U\} = \{F\} \quad (2.1)$$

in which $[K]$ denotes the ‘overall stiffness matrix’ of the body. The ‘overall force vector’ $\{F\}$ list the externally applied forces at all the nodes, while $\{U\}$ list the displacement of all the nodes. Throughout this study $[]$ and $\{ \}$ will denote square (or rectangular) matrices and vectors respectively.

An inspection of Equation 2. 1 shows that, qualitatively, $[K]$ represent the force required to produce unit displacement of the finite element model of the body as an equivalent ‘spring’, then $[K]$ will obviously be a ‘spring constant’ representing its ‘stiffness’. Thus, the finite element method is essentially one in which the analysis of the body is carried out from the point of view of its ‘stiffness’.

For a given set of prescribed boundary conditions and external forces acting on the body, Equation 2. 1 can be solved uniquely for the nodal displacement, $\{U\}$, from which the stresses and strain within the body can subsequently be computed.

To summaries, the finite element solution of a given problem will require the execution of the following operation in this order:

1. Discretization (subdivision) of the body into a system of finite elements.
2. Derivation of the element stiffness matrix and other properties for each individual element representing the body.
3. Assembly of the overall stiffness matrix $[K]$ and overall force vector $\{F\}$.
4. Solution of Equation 2. 1 with prescribed boundary conditions to determine $\{U\}$, and

5. Calculation of stresses and strains within the elements from the computed nodal displacement, $\{ \}$.

2.2. Why the Finite Element Method ?

Why should anyone use the Finite Element method in preference to other numerical methods, in particular to the Finite Difference method which after all is well founded, older and reliable? The main points in favor of the finite element method over other methods are these:

1. Owing to the flexibility of their sizes and shapes, finite element are able to represent a given body, however complex its shape may be, more faithfully.
2. Multiply-connected domains (i.e., bodies with one or more holes in them) or those with corners Figure 2. 3 can be dealt without difficulty.
3. Problems involving variable material properties and/or variable geometry, do not present any additional difficulty. Geometrical and material non-linearities, even hereditary (i.e. time-dependent) material properties can be dealt with relatively easily.
4. Problems of cause-effect relationships are formulated in terms of generalized 'forces' and 'displacements' which are related trough to overall stiffness matrix.

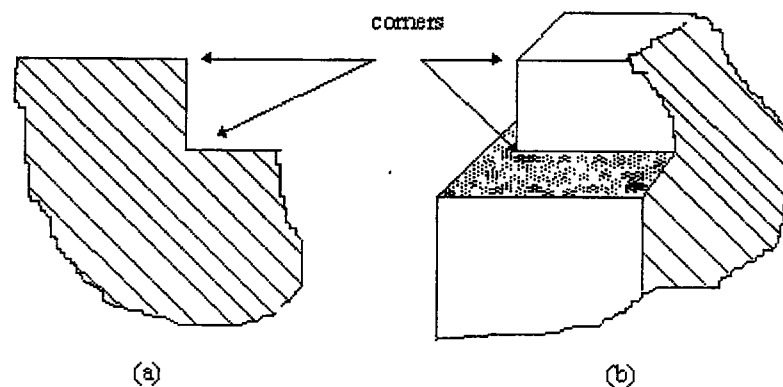


Figure 2. 3 Corners in (a) two dimensions and (b) in three dimensions.

This aspect of the finite element method facilitates and indeed simplifies the understanding of the problem and its solution.

5. Boundary condition are easily dealt with.
6. The versatility and flexibility of the finite element method can be used very effectively to evaluate the cause-effect relationships in complex structural, continuum, field and other problems. Resulting accuracy is well comparable and often better than those arrived at via other analytical (if possible) or experimental methods.

2.3. Finite Element Meshes

It would have been observed that it is an easy matter to obtain a coarse subdivision of the analysis domain with a small number of isoparametric elements.

The main drawback of the mapping and generation suggested is the fact that the originally circular boundaries in Figure 2. 4 are approximated by simple parabola and a geometric error can be developed for representation of complex motor car body shapes, can be adopted for this purpose. If the coordinates x and y are used by interpolation or shape function in local coordinates, then any complex can be mapped by any single element. The region of Figure 2. 4 in fact so mapped and a mesh subdivision obtained directly without any geometry error on the boundary.

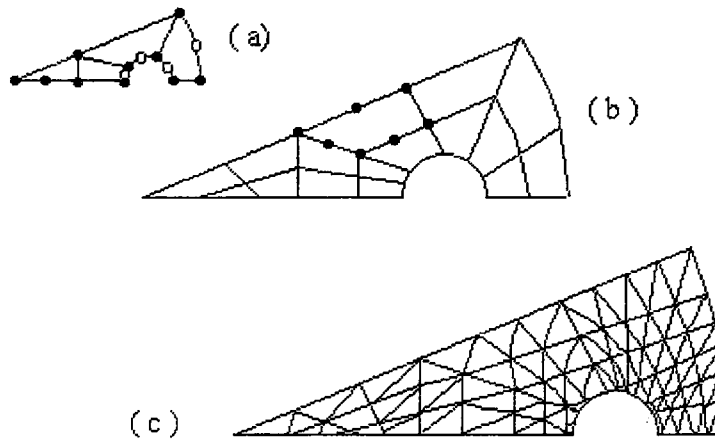


Figure 2. 4 Automatic mesh generation by parabolic isoparametric elements. (a) Specified mesh points (b) Automatic subdivision into small number of isoparametric elements.(c) Automatic subdivision into linear triangles.

2.4. The Isoparametric Elements

The isoparametric formulation makes it possible to generate elements that are nonrectangular and have curved sides. These shapes have obvious uses in grading a mesh from coarse to fine, in modeling arbitrary shapes, and in modeling curved boundaries Figure 2. 5. The isoparametric family includes elements for plane, solid, plate, and shell problems. In the following isoparametric elements, natural coordinate system must be used (system ξ , η and ξ , η , t in Figure 2. 6. Displacements are expressed in terms of natural coordinates, but must be differentiated with respect to global coordinates x , y and z .

Accordingly, a transformation matrix must be obtained. In addition, integrations must be done numerically rather than analytically if elements are nonrectangular.

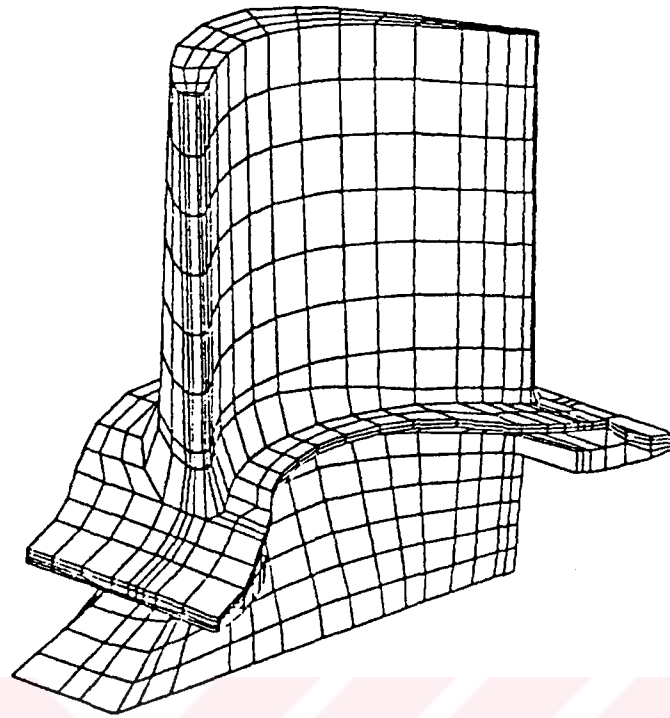


Figure 2. 5 Turbine blade, modeled by solid elements.

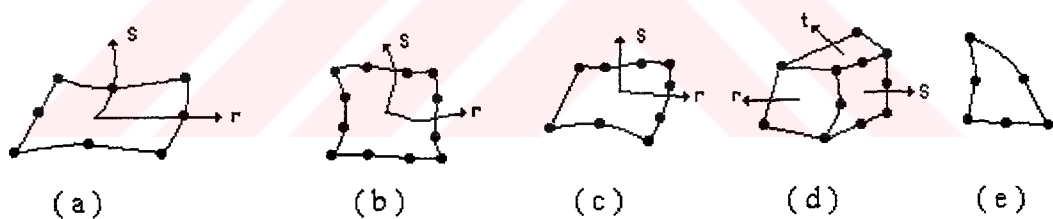


Figure 2. 6 Isoparametric elements (a) Quadratic plane element. (B) Cubic plane element. (a) A degraded cubic element, the left and lower sides can be joined to linear quadratic element. (d) Quadratic solid element with some linear edges. (e) A quadratic plane triangle

The term isoparametric means same parametric. In other words, the degree of interpolation on coordinates are the same on displacements. Elements with a higher degree of interpolation on coordinates than on displacements are called superparametric. If the coordinates are interpolated to a lower degree than the displacements, elements are called subparametric.

An important consideration in the global coordinate system. In this regard, three useful guidelines have been advanced :

1. If two adjacent curved elements are generated from parent elements whose interpolation function satisfy interelement continuity, these curved isoparametric elements will be continuous.
2. If the interpolation function are given in the local coordinate system and they are continuous in the parent element, will also be continuous in the curved isoparametric element.
3. The isoparametric element formulation offers the attractive feature that, if the completeness criterion is satisfied in the parent element, it is automatically satisfied in the curved isoparametric element.

2.5. Interpolation Function

In the finite element literature, the functions used to represent the behavior of a field variable within an element are called interpolation functions, shape functions, or approximating functions. Although it is conceivable that many types of functions could serve as interpolation functions, only polynomials have received widespread use. The reason is that polynomials are relatively easy to manipulate mathematically, in other words, they can be integrated or differentiated without difficulty. Trigonometric functions also possess this property, but they are seldom used. Ignored for the moment any interelement continuity considerations, we can say that the order of the polynomial we use to represent the field variable within an element depends on the number of degrees of freedom we assign to the element. In other words, the number of coefficients in the polynomial should equal the number of nodal variables available to evaluate these coefficients.

We could not expect a good approximation to reality if our field variable representation changed with a change in origin or in the orientation of the coordinate system. Hence the need to ensure geometric isotropy in our polynomial series with the desired property:

1. Polynomials of order n that are complete have geometric isotropy.
2. Polynomials of order n that are incomplete, yet contain the appropriate terms to preserve symmetry, have geometric isotropy.

There are three types of polynomials:

1. One independent variable
2. Two independent variable
3. Three independent variable

Here only two independent variable will be given.

2.6. Two Independent Variable

In two dimensions a complete nth-order polynomial may be written as

$$P_n(x,y) = \sum_{k=1}^{T_n} \alpha_k x^i y^j, \quad i + j \leq n \quad (2.2)$$

where the number of terms in the polynomial is

$$T_n = (n + 1)(n + 2) / 2 \quad (2.3)$$

second- order polynomials with two independent variable are given as

$$P_2(x,y) = \alpha_1 + \alpha_2 x + \alpha_3 y + \alpha_4 xy + \alpha_5 x^2 + \alpha_6 y^2 \quad (2.4)$$

2.7. Interpolation Functions Of Rectangular Elements

Interpolation functions have been developed for one, two, and three dimensional elements. Here only two dimensional interpolation function will be shown for rectangular element. The basic ideas can be illustrated by a simple example in two dimensions. Suppose that we wish to construct a rectangular element with nodes positioned at the corners of the element Figure 2. 7.a. If we assign one value of interpolation to each node, the element then has four degrees of freedom, and we may select as an interpolation model a four-term polynomial such as

$$P(x,y) = \alpha_1 + \alpha_2 + \alpha_3 y + \alpha_4 xy \quad (2.5)$$

and for rectangular element with eight nodes Figure 2.7.b, a eight-term polynomial is chosen as

$$P(x,y) = \alpha_1 + \alpha_2 + \alpha_3 y + \alpha_4 xy + \alpha_5 x^2 + \alpha_6 y^2 + \alpha_7 x^2y + \alpha_8 xy^2 \quad (2.6)$$

2.8. Natural Coordinates

A local coordinate system that relies on the element geometry for its definition and whose coordinates range between zero and unity within the element is known as a natural coordinate system. Such systems have the property that one particular coordinate has unit value at one node of the element and zero value at the other node(s). We may construct natural coordinate system for two-node line elements, three-node triangular elements, four-node rectangular elements, and so on into n-dimensional hyperspace. Natural coordinates in n dimensions are called barycentric coordinates.

The basic purpose of the natural coordinate system is to describe the location of a point inside an element in terms of coordinates associated with the nodes of the element. It will become evident that the natural coordinates are functions of the global Cartesian coordinates system in which the element is defined.

Here only natural coordinate will be shown for a four-node quadrilateral element in two dimensions. Figure 2.8 shows a general quadrilateral element in the global Cartesian coordinates system and local natural coordinate system. In the natural coordinate system whose origin is at the centroid the quadrilateral element is a square with sides extending $\xi = \pm 1, \eta = \pm 1$.

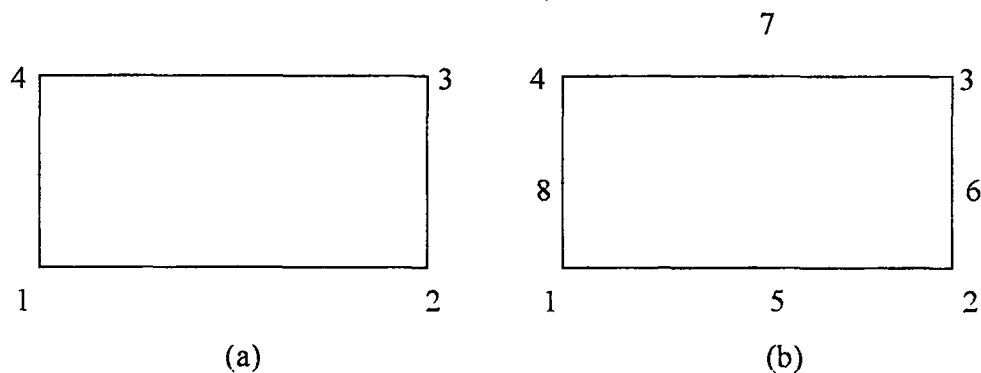


Figure 2.7 Rectangular element (a) Four-node element, (b) Eighth-node element

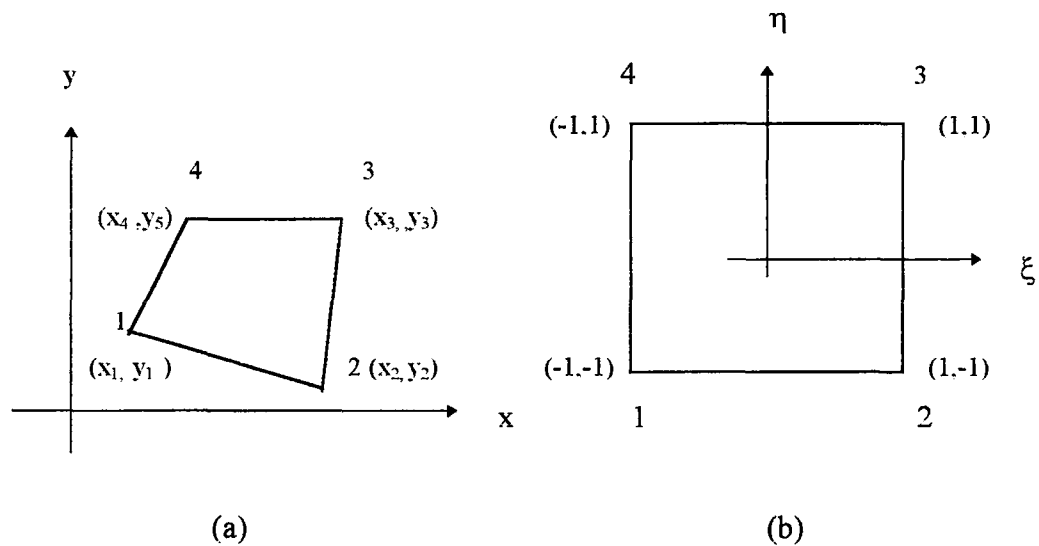


Figure 2. 8 Natural coordinates for a general quadrilateral.(a) Cartesian coordinates
(b) Natural coordinates

The local and global coordinates are related by the following equations:

$$x = \frac{1}{4} [(1-\xi)(1-\eta)x_1 + (1+\xi)(1-\eta)x_2 + (1-\xi)(1+\eta)x_3 + (1+\xi)(1+\eta)x_4] \quad (2.7)$$

$$y = \frac{1}{4} [(1-\xi)(1-\eta)y_1 + (1+\xi)(1-\eta)y_2 + (1-\xi)(1+\eta)y_3 + (1+\xi)(1+\eta)y_4] \quad (2.8)$$

2.9. Lagrange Polynomials

One type of useful interpolation function is the Lagrange polynomial, defined as

$$L_k(x) = \sum_{\substack{m=0 \\ m \neq k}}^n \frac{x-x_m}{x_k-x_m} = \frac{(x-x_0)\dots(x-x_{k-1})(x-x_{k+1})\dots(x-x_n)}{(x_k-x_0)\dots(x_k-x_{k-1})(x_k-x_{k+1})\dots(x_k-x_n)} \quad (2.9)$$

Since $L_k(x)$ is a product of n linear factor, it is clearly a polynomial of degree n . We note that, $x=x_k$, the numerator and denominator of $L_k(x_k)$ are identical and the polynomial has unit value. But when $x=x_m$ and $m \neq k$, the polynomial vanishes. This fact can be used to represent an arbitrary function $\varnothing(x)$ over an interval on the x axis. For example, suppose that $\varnothing(x)$ is given by discrete values at four points in the closed interval $[x_0, x_3]$ Figure 2.

9a. A polynomial at degree 3 passing through the four discrete values $\phi_i = \phi(x_i)$ ($i=0,1,2,3$) and approximating the function $\phi(x)$ in the interval may be written at once as

$$\Phi(x) = \sum_{i=0}^3 \phi_i L_i(x) = [L] \{\Phi\} \tag{2.10}$$

and we recognize that $L_i(x)$ plays the role $N_i(x)$.

The Lagrange polynomials L_i in the expression for $\phi(x)$ are sometimes called lagrangian interpolation coefficients. Figure 2. 9b shows how these coefficient for ϕ_2 , for instance, would become

$$L_1(x) = \frac{(x-x_0)(x-x_2)(x-x_3)}{(x_1-x_0)(x_1-x_2)(x_1-x_3)} \tag{2.11}$$

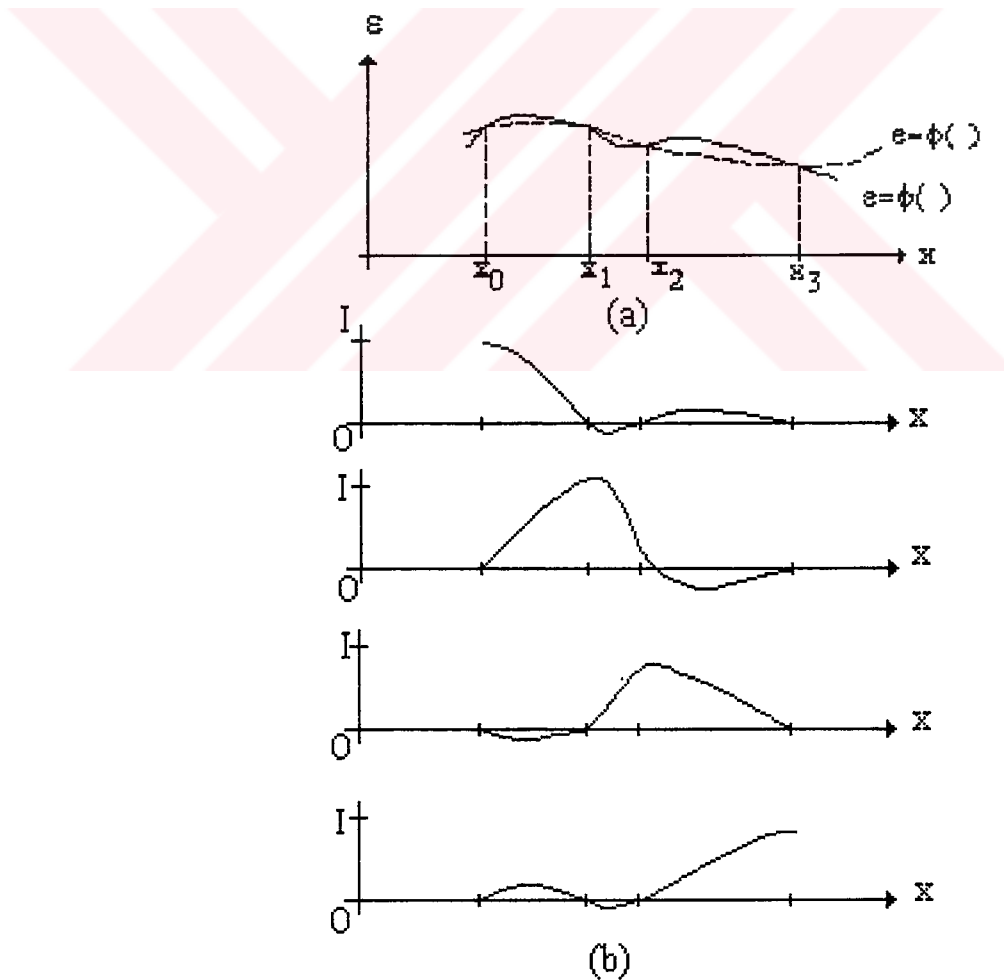


Figure 2. 9 Interpolation using Lagrange polynomials (a) The given function and its approximate representation, (b) Lagrange Interpolation coefficients.

Since the lagrangian coefficients possess the desired properties of the nodal interpolation functions, we may write immediately for any line element within only \mathcal{O}_1 , specified at the nodes.

$$N_i(x) = L_i(x) \quad (2.12)$$

With the order of the interpolation polynomials depending on the number of nodes we assign to the element. Since lagrangian interpolation function guarantee continuity of \mathcal{O} at the connecting nodes, they are suitable for elements used in problems requiring C^0 continuity.

2.10. Obtaining The Interpolation Function

2.10.1. For The Isoparametric Finite Element Matrices:

In this study, Lagrange polynomials are chosen as the interpolation functions. In the plane stress case, each nodal point has two coordinates, x and y, and two displacement, u and v, they are obtained for the rectangular elements with nine nodes Figure 2. 10 in this form;

$$x = \sum_{i=1}^9 N_i x_i, \quad y = \sum_{i=1}^9 N_i y_i \quad (2.13)$$

$$u = \sum_{i=1}^9 N_i u_i, \quad v = \sum_{i=1}^9 N_i v_i$$

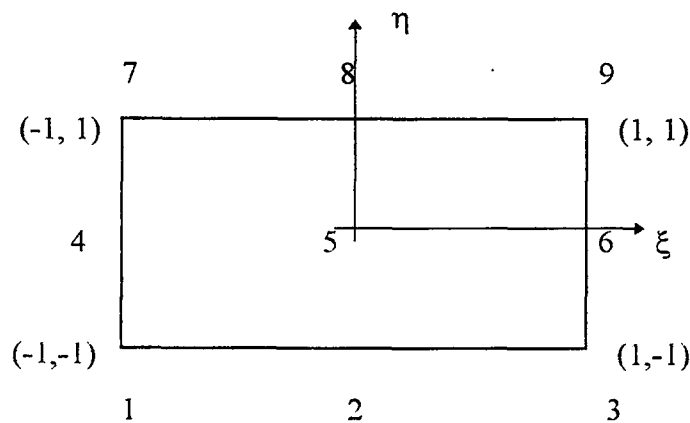


Figure 2. 10 The rectangular isoparametric element

Interpolation functions written as,

$$\begin{aligned}
 N_1(\xi, \eta) &= L_1(\xi).L_1(\eta) \\
 N_2(\xi, \eta) &= L_2(\xi).L_1(\eta) \\
 N_3(\xi, \eta) &= L_3(\xi).L_1(\eta) \\
 N_4(\xi, \eta) &= L_1(\xi).L_2(\eta) \\
 N_5(\xi, \eta) &= L_2(\xi).L_2(\eta) \\
 N_6(\xi, \eta) &= L_3(\xi).L_2(\eta) \\
 N_7(\xi, \eta) &= L_1(\xi).L_3(\eta) \\
 N_8(\xi, \eta) &= L_2(\xi).L_3(\eta) \\
 N_9(\xi, \eta) &= L_3(\xi).L_3(\eta)
 \end{aligned} \tag{2.14}$$

and Lagrange polynomials are obtained in the following form;

$$\begin{aligned}
 L_1(\xi) &= -\frac{1}{2} \xi (1-\xi) \\
 L_2(\xi) &= (1+\xi) (1-\xi) \\
 L_3(\xi) &= -\frac{1}{2} \xi (1+\xi)
 \end{aligned} \tag{2.15}$$

and $L_1(\eta)$, $L_2(\eta)$, $L_3(\eta)$ are obtained similarly, substituting η instead of ξ . Lagrange polynomials are second- order polynomials that pass through three nodal points.

2.11. Obtaining The Element Properties

In the plane stress case, the strain-displacement relations are written as

$$\epsilon_x = \frac{\partial u}{\partial x} \quad , \quad \epsilon_y = \frac{\partial v}{\partial y} \quad , \quad \gamma_{xy} = \frac{\partial u}{\partial y} + \frac{\partial v}{\partial x} \tag{2.16}$$

and derivatives of u and v with respect to x and y are obtained the following form;

$$\begin{aligned} \frac{\partial u}{\partial x} &= \sum_{i=1}^9 \frac{\partial N_i}{\partial x} u_i \quad ; & \frac{\partial v}{\partial x} &= \sum_{i=1}^9 \frac{\partial N_i}{\partial x} v_i \\ \frac{\partial u}{\partial y} &= \sum_{i=1}^9 \frac{\partial N_i}{\partial y} u_i \quad ; & \frac{\partial v}{\partial y} &= \sum_{i=1}^9 \frac{\partial N_i}{\partial y} v_i \end{aligned} \quad (2.17)$$

Consider for instance the set of local coordinates ξ, η and a corresponding set of global coordinates x, y . By the usual rule of partial differentiation we can write instance ξ, η derivatives as

$$\begin{aligned} \frac{\partial N_i}{\partial \xi} &= \frac{\partial N_i}{\partial x} \cdot \frac{\partial x}{\partial \xi} + \frac{\partial N_i}{\partial y} \cdot \frac{\partial y}{\partial \xi} \\ \frac{\partial N_i}{\partial \eta} &= \frac{\partial N_i}{\partial x} \cdot \frac{\partial x}{\partial \eta} + \frac{\partial N_i}{\partial y} \cdot \frac{\partial y}{\partial \eta} \end{aligned} \quad (2.18)$$

Writing in matrix form we have

$$\begin{Bmatrix} \frac{\partial N_i}{\partial \xi} \\ \frac{\partial N_i}{\partial \eta} \end{Bmatrix} = \begin{bmatrix} \frac{\partial x}{\partial \xi} & \frac{\partial y}{\partial \xi} \\ \frac{\partial x}{\partial \eta} & \frac{\partial y}{\partial \eta} \end{bmatrix} \begin{Bmatrix} \frac{\partial N_i}{\partial x} \\ \frac{\partial N_i}{\partial y} \end{Bmatrix} = \mathbf{J} \begin{Bmatrix} \frac{\partial N_i}{\partial x} \\ \frac{\partial N_i}{\partial y} \end{Bmatrix} \quad (2.19)$$

In the above, the left-hand side can be evaluated as the functions N_i are specified in local coordinates. Further as x, y are explicitly given by the relation defining the curvilinear coordinates Equation 2. 13, the matrix \mathbf{J} can be found explicitly in terms of the local coordinates. This matrix is known as the Jacobian matrix.

Inverting \mathbf{J} we can write

$$\begin{Bmatrix} \frac{\partial N_i}{\partial x} \\ \frac{\partial N_i}{\partial y} \end{Bmatrix} = \mathbf{J}^{-1} \begin{Bmatrix} \frac{\partial N_i}{\partial \xi} \\ \frac{\partial N_i}{\partial \eta} \end{Bmatrix} \quad (2.20)$$

We can obtain J^{-1} in the following form

$$J^{-1} = \frac{1}{\det J} \begin{bmatrix} \frac{\partial y}{\partial \xi} & -\frac{\partial x}{\partial \xi} \\ -\frac{\partial y}{\partial \eta} & \frac{\partial x}{\partial \eta} \end{bmatrix} \quad (2.21)$$

and

$$\det J = \frac{\partial x}{\partial \xi} \cdot \frac{\partial y}{\partial \eta} - \frac{\partial x}{\partial \eta} \cdot \frac{\partial y}{\partial \xi} \quad (2.22)$$

We obtain the properties of the Jacobian as

$$\frac{\partial x}{\partial \xi} = \sum_{i=1}^9 \frac{\partial N_i}{\partial \xi} x_i = \left\{ \frac{\partial N_i}{\partial \xi} \dots \right\} x_i$$

$$\frac{\partial y}{\partial \xi} = \sum_{i=1}^9 \frac{\partial N_i}{\partial \xi} y_i = \left\{ \frac{\partial N_i}{\partial \xi} \dots \right\} y_i$$

$$\frac{\partial x}{\partial \eta} = \sum_{i=1}^9 \frac{\partial N_i}{\partial \eta} x_i = \left\{ \frac{\partial N_i}{\partial \eta} \dots \right\} x_i$$

$$\frac{\partial y}{\partial \eta} = \sum_{i=1}^9 \frac{\partial N_i}{\partial \eta} y_i = \left\{ \frac{\partial N_i}{\partial \eta} \dots \right\} y_i$$

(2.23)

We can rewrite Equation 2.16 in the matrix form as

$$\{\varepsilon\} = \begin{Bmatrix} \varepsilon_x \\ \varepsilon_y \\ \gamma_{xy} \end{Bmatrix} = \begin{Bmatrix} \frac{\partial u}{\partial x} \\ \frac{\partial v}{\partial y} \\ \frac{\partial u}{\partial y} + \frac{\partial v}{\partial x} \end{Bmatrix} = [B] \{U\} \quad (2.24)$$

where

$$B = \begin{bmatrix} \frac{\partial N_i}{\partial x} & 0 \\ 0 & \frac{\partial N_i}{\partial y} \\ \frac{\partial N_i}{\partial y} & \frac{\partial N_i}{\partial x} \end{bmatrix} \quad (2.25)$$

and

$$\{U\} = \{u_1 \ v_1 \ u_2 \ v_2 \dots u_n \ v_n\}^T \quad (2.26)$$

The system equations are obtained by the minimum potential energy principle as,

$$[K] \{U\} = \{F\} \quad (2.27)$$

where

$$[K] = \int_{-1}^1 \int_{-1}^1 [B]^T [C] [B] dV \quad (2.28)$$

In plane stress case, volume element dV can be written as

$$dV = t \, dx \, dy \quad (2.29)$$

and

$$dx \, dy = \det J \, d\xi \, d\eta \quad (2.30)$$

In this case, we rewrite the stiffness matrix as

$$[K] = t \int_{-1}^1 \int_{-1}^1 [B]^T [C] [B] \det J \, d\xi \, d\eta \quad (2.31)$$

where

$$[C] = \frac{E}{1-\nu^2} \begin{bmatrix} 1 & \nu & 0 \\ \nu & 1 & 0 \\ 0 & 0 & \frac{1-\nu}{2} \end{bmatrix} \quad (2.32)$$

2.12. Calculation of Elasto-Plastic Stresses

Various computational procedures have been used with success for a limit range of elasto-plastic problems utilizing the finite element approach. Two main formulations appear. In the first, during an increment of loading, the increase of plastic strain is computed and treated as an *initial strain* for which the elastic stress distribution is adjusted. This approach manifestly fails in ideal plasticity is postulated or if the hardening is small. The second approach is that in which the stress-strain relationship every load increment is adjusted to take into account plastic deformation. With properly specified elasto plastic matrix this incremental elasticity approach can successfully treat ideal as well as hardening plasticity.

From the computational point of view the incremental elasticity process has one serious disadvantage. At each step of computation the stiffness of the structure is changed and iterative process of solution are necessary to avoid excessive computer times. The initial stress method

is developed by Zienkiewicz as an alternative approach to the incremental elasticity process. By using the fact that even in ideal plasticity increments of strain prescribe uniquely the stress system (while the reverse is not true for ideal plasticity) an adjustment process is derived in which initial stresses are distributed elastically through the structure.

This approach permits the advantage of initial process (in which the basic elasticity matrix remains unchanged) to be retained. The process appears to be the most rapidly convergent. To start elasto-plastic stress analysis, this method uses one dimensional tensile specimen in elasto-plastic region, then moves on to the two and three dimensional stress case. For a tensile specimen loaded just over the elastic region ($\epsilon_{total} = \epsilon_1$). Stress σ_x is calculated linear elasticity, thus the stress σ_{f1} as shown in Figure 2. 11 below is given by the following form ;

$$\sigma_{01} = \sigma_x - \sigma_{f1} = \sigma_1 - \sigma_{f1} \quad (2.33)$$

By using σ_{01} one obtains increasing stress value

$$\sigma_2 = \sigma_x + \sigma_{01} \quad (2.34)$$

which corresponding to ϵ_2 . The stress difference between σ_2 and real stress at ϵ_2 gives σ_{02} . σ_3 is obtained by replacing σ_{02} in Equation 2. 34. The following analog iteration steps lead to the point corresponding to the elasto-plastic strain ϵ_n and stress σ_x . Where σ_{oi} is the initial stress.

For calculation of stress in two dimensional cases equivalent stress is usually obtained according to Von Misses criterion (Distortion energy theory).The equivalent stress in plane stress case is

$$\bar{\sigma} = \{0.5((\sigma_x - \sigma_y)^2 + \sigma_x^2 + \sigma_y^2) + 3\tau_{xy}^2\}^{1/2} \tag{2.35}$$

Where σ_x , σ_y , and τ_{xy} are the stress components.

Therefore initial stress can be obtained for plastic region is one dimensional case,

$$\sigma_0 = \bar{\sigma} - \sigma_f \tag{2.36}$$

where σ_f is obtained from σ , ϵ_{total} diagram a uniaxially loaded tensile specimen. But the initial stress cannot be exactly described as in Figure 2. 11 in two dimensional case. It can be mathematically described as follows,

$$\{\sigma_0\} = \{\sigma_{0x} \ \sigma_{0y} \ \tau_{0xy}\} \tag{2.37}$$

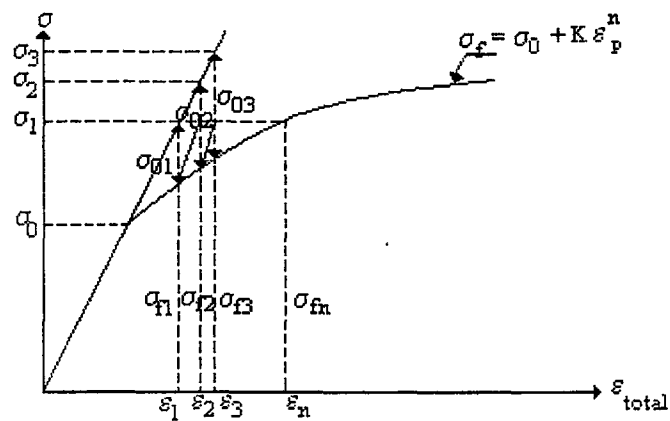


Figure 2. 11 Representation of initial stress method

where σ_{0x} , σ_{0y} and τ_{0xy} are components of the initial stress in plane stress case. By using the following formal, one obtains

$$\{\sigma_0\} = \{\sigma\} \{\sigma_0 / \bar{\sigma}\} \quad (2.38)$$

where the component of $\{\sigma_0\}$ are proportional to elastically calculated stress. The related equivalent stress value is equal to $\{\sigma_0\}$ obtained in one dimensional case, according to Equation 2.33

$$\bar{\sigma} = \left\{ \frac{1}{2} [(\sigma_{0x} - \sigma_{0y})^2 + \sigma_{0x}^2 + \sigma_{0y}^2] + 3\tau_{oxy}^2 \right\}^{\frac{1}{2}} \quad (2.39)$$

The loading corresponding to the initial stress as follows;

$$\{F\} = \int_v [B]^T \{\sigma_0\} dV \quad (2.40)$$

First the solution vector is calculated for $\{F\}_{\sigma_{01}}$, mechanical loading in the first iteration step

$$\{\delta\}_1 = [K]^{-1} \{F\}_m \quad (2.41)$$

where $\{F\}_m = \{F\}_s + \{F\}_{\sigma_0}$ then the following iteration steps $\{\delta\}_i$, $i=1, 2, \dots, n$ are calculated until there is no difference between $\{\delta\}_i$ and $\{\delta\}_{i+1}$. Then the displacement vector is

$$\{\delta\}_n = [K]^{-1} \{F\}_m \quad (2.42)$$

Finally the stress σ_n corresponding to $\{\delta\}_n$ in elasto-plastic region is calculated as

$$\{\sigma\}_n = [C][B]\{\delta\}_n \quad (2.43)$$

In the elasto-plastic region, residual stresses are found at the end of iteration as follows,

$$\{\sigma_{0i}\} = [\{\sigma\}_L - \{\sigma\}_n] \quad (2.44)$$

where, $\{\sigma\}_L$ is the linear elastic stress obtained at the end of iteration. In the polar coordinates, residual stresses are written as,

$$\{\sigma_{0i}\}_{pc} = [T] \{\sigma_{0i}\} \quad (2.45)$$

where

$$[T] = \begin{bmatrix} \cos^2\theta & \sin^2\theta & 2\sin\theta \cdot \cos\theta \\ \sin^2\theta & \cos^2\theta & -2\sin\theta \cdot \cos\theta \\ -\sin\theta \cdot \cos\theta & \sin\theta \cdot \cos\theta & \cos^2\theta - \sin^2\theta \end{bmatrix} \quad (2.46)$$

is transformation matrix.



CHAPTER THREE

ANALYSIS OF COMPOSITE MATERIALS

3.1 Introduction

Composite materials are ideal for structural applications where high strength-to weight and stiffness-to-weight ratios are required. Aircraft and spacecraft are typical weight-sensitive structures in which composite materials are cost-effective. When the full advantages of composite materials are utilized, both aircraft and spacecraft will be designed in a manner much different from present.

For isotropic materials, normal stress causes extension in the direction of the applied stress and contraction in the perpendicular direction. Also, shear stress causes only shearing deformation.

For orthotropic materials, like isotropic materials, normal stress in a principal material direction (along one of the intersection of three orthogonal planes of material symmetry) results in extension in the direction of the applied stress and contraction perpendicular to the stress. However, due to different properties in the two principal material directions, the contraction can be either more or less than the contraction of a similarity loaded isotropic material with the same elastic modules in the direction of the load. Shear stress causes shearing deformation, but the magnitude of the deformation is independent of the various Young's moduli and the Poisson's ratios. That is, the shear modules of an orthotropic material is, unlike isotropic materials, not depend on other material properties.

3.2 Properties of Composite Materials

3.2.1 Fibrous Composites

A fiber is characterized geometrically not only by its very high length-to-diameter ratio but by its near crystal-sized diameter. Strengths and stiffness of a few selected fiber materials are shown in Table 3. 1. Many common materials are listed for the purpose of

comparison. Note that the density of each material is listed since the strength-to-density and stiffness-to-density

Table 3. 1 Fiber and wire properties

Fiber or wire	Density ρ (kN/m ³)	Tensile strength S(GN/m ²)	S/ ρ (10 ³ m)	Tensile stiffness E (GN/m ²)	E/ ρ (10 ⁶ m)
Aluminum	26.3	0.62	24	73	2.8
Titanium	46.1	1.9	41	115	2.5
Steel	76.6	4.1	54	207	2.7
E-glass	25.0	3.4	136	72	2.9
S-glass	24.4	4.8	197	86	3.5
Carbon	13.8	1.7	123	190	14
Beryllium	18.2	1.7	93	300	16
Boron	25.2	3.4	137	400	16
Graphite	13.8	1.7	123	250	18

ratios are commonly used as indicators of the effectiveness of a fiber, especially in weight-sensitive applications such as aircraft and space vehicles. Entries in Table 3. 1 are arranged in increasing average S/ ρ and E/ ρ .

3.2.2 Properties of Matrices

Naturally, fibers and whiskers are of little use unless they are bound together to take the form of a structural element which can take loads. The binder material is usually called a matrix. The purpose of the matrix is manifold: support, protection, stress transfer, etc. Typically, the matrix is of considerably lower density, stiffness, and strength than fibers or whiskers. However, the combination of fibers or whiskers and a matrix can have very high strength and stiffness, yet still have low density.

3.3 Laminae

A lamina is a flat (some times curved as in a shell) arrangement of unidirectional fibers or woven fibers in a matrix. Two typical laminae are shown in figure below along with their principal material axes which are parallel and perpendicular to the fiber directions. The fibers, or filaments, are the principal reinforcing or load-carrying agent. They typically strong and stiff. The matrix can be organic, ceramic, or metallic. The function of the matrix is to support and protect the fibers and to provide a means of distributing load among and transmitting load between the fibers.

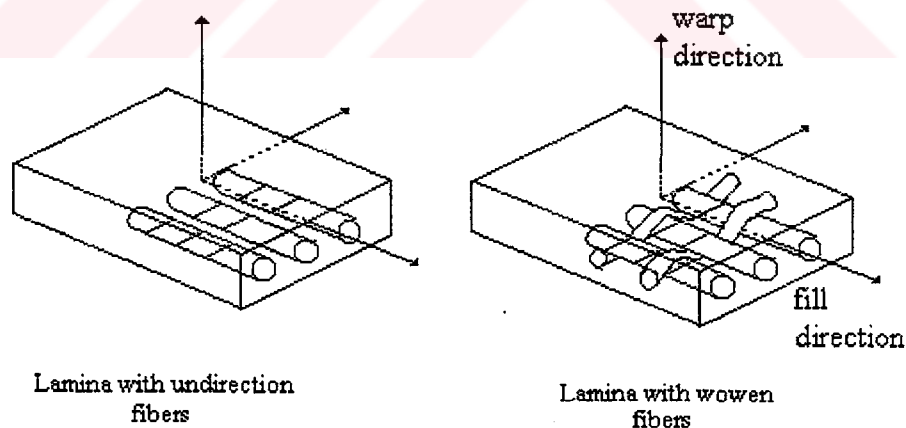


Figure 3. 1 Two principal types of laminae

The latter function is especially important if a fiber breaks as figure below. There, load from one side of a broken fiber as well as to adjacent fibers. The mechanism for the load transfer is the shearing stress developed in the matrix; the shearing stress the pulling out of

the broken fiber. This load-transfer mechanism is the means by which whisker-reinforced composites carry any load at all above the inherent matrix strength.

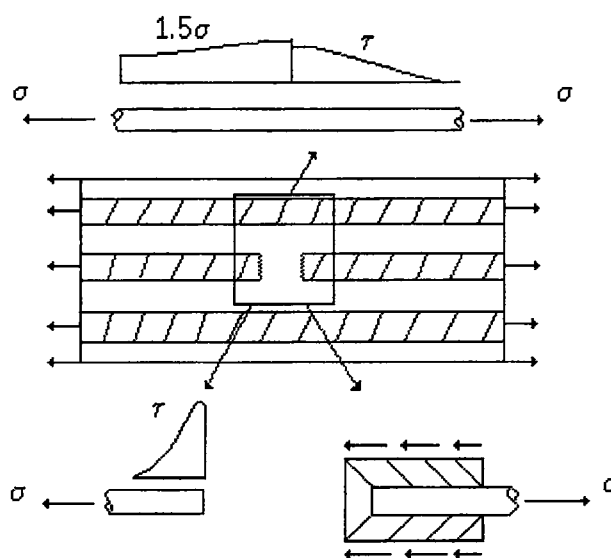


Figure 3. 2 Effect of broken fiber on matrix and fiber stresses

3.4 Laminates

A laminate is a stack of laminae with various orientations of principal material directions in the laminae as in figure below. Note that the fiber orientation of the layers in this figure is not symmetric about the middle surface of the laminate. This situation will be discussed in following pages. The layers of a laminate are usually bound together by the same matrix material that is used in the laminae. Laminates can be composed of plates of different materials or, in the present context, layers of fiber-reinforced laminae. A laminated circular cylindrical shell can be constructed by winding resin-coated fibers on a mandrel first with one orientation to the shell axis, then another, and so until the desired thickness is built up.

A major purpose of lamination is to tailor the directional dependence of strength and stiffness of a material to match the loading environment of the structural element. Laminates are uniquely suited to this objective since the principal material directions of each layer can be oriented according to need. For example, six layers of a ten-layer laminate could be oriented in one direction and the other four at 90° to that direction; resulting laminate then has a strength and extensional stiffness roughly 50 percent higher in one direction than the other. The ratio of the extensional stiffness in the two directions is

approximately $6/4$, but the ratio of bending stiffness is unclear since the order of lamination is not specified in the example. Moreover, if the laminae are not arranged symmetrically about the middle surface of the laminate, stiffness exist that describe coupling between bending and extension. These characteristics will be discussed in following pages.

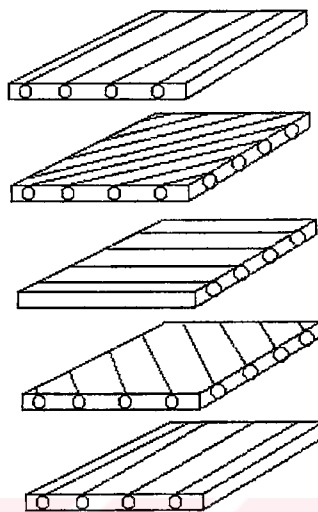


Figure 3. 3 Laminate Construction

A potential problem in the construction of laminates is the introduction of shearing stresses between layers. The shearing stresses arise due to the tendency of each layer to deform independently of its neighbors because all may have different properties (at least from the standpoint of orientation of principal material directions). Such shearing stresses are largest at the edges of a laminate and may cause delimitation there. As will be shown in following pages the transverse normal stress can also cause delimitation.

3.5 Metal Matrix Composite Materials

The technology of metal-matrix composite materials is being developed very rapidly. Compared to glass-fiber-reinforced plastics, metal-matrix composites are superior for their performance at elevated temperatures. The strength and elastic moduli of metal matrices are higher than those resin matrices over a wide range of temperature. As to deformation of the composites, metal matrices can greatly enhance the ductility of the composite. The stress concentrations induced by cracked fibers can be relaxed through the plastic deformation of matrix. As a result there is less chance of a brittle failure of the composite. The majority of the load applied to a metal matrix composite is carried by the reinforcing fibers. Since the

metal matrices are strong in shear strength and, in general, well bonded to fibers, short fibers can be used effectively for the purpose of strengthening. An obvious disadvantage of this type of composites is their relatively high density.

3.6 Fabrication Methods for Metal-Matrix Composites

In this section the methods used for fabricating metal-matrix composites are briefly. These methods serve first to combine the fiber and matrix materials and then to consolidate the combination to form the desired shape of the end-product.

a) Powder Metallurgy Technique

The technique of powder metallurgy involves the compacting of solid materials in the form of powders. The powder process has been used for ceramic as well as metallic materials. The product resulting from the powder process is uniform in composition, in contrast to alloys produced by casting. In the latter case, segregation of the component phases often occurs during solidification, and homogenization of the alloy is needed. Since no melting or casting involved, the powder process is more economical than many other fabrication techniques. In this process, powders of ceramics or metals are first prepared and then fed into a mold of desired shape. Pressure is then applied to further compact the powder. In order to facilitate the bonding among powder particles, the compact is often heated to a temperature which is below the melting point but high enough to develop significant solid state diffusion. The use of heat to bond solid particles is known as sintering or firing. There is no separate bonding phase generated in the sintering process. Through diffusion, the point of contact between two neighboring particles develops into a surface and the bonding between them is hence strengthened. The driving force for sintering is the elimination of particle surface area.

Metallic materials such as copper, nickel, aluminum, cobalt, and steel are often used in the powder process as matrix materials. The metal matrices in the form of powders are first mixed with whiskers or copped fibers. The combination is then consolidated by pressing, sintering, hot extrusion, or rolling, in order to enhance the density and strength of the

composite. The exposure to high temperature and pressure for long periods may be detrimental to some composite systems.

b) Liquid Metal Infiltration

Metal such as aluminum, magnesium, silver, and copper have been used as matrix materials in this process because of their relatively lower melting points. The method of liquid metal infiltration is desirable in producing relatively small size composite specimens. Fibers collimated in a mold are infiltrated with liquid metal. By employing the idea of liquid metal infiltration, it is possible to cast composite structures such as rods and beams by passing a bundle of filaments through a liquid-metal bath in a continuous manner. Structures solidified in this manner have uniform cross-sections with uniaxial reinforcement, and need little additional work. The application of the liquid-metal infiltration process is limited by the available choice matrix and reinforcing materials. The degradation of many fibers at high temperatures rules out their use. Another consideration is the wetting of reinforcements by the liquid metal. This problem will not be discussed in this study.

c) Diffusion Bonding

Just as in the case of sintering, the diffusion bonding process is carried out under high pressure and elevated temperature. Filaments of stainless steel, boron, and silicon carbide have been used with matrices such as aluminum and titanium alloys. Unlike the powder process, the matrix metals used in most commercially available composites are in the form of metal foils. In order to fully develop the bonding strength among the foils and between the foil and the fiber, they all have to be thoroughly cleansed. The fibers are then laid on the metal sheets in predetermined spacing and orientation. Alternate layers of metal foils and reinforcing fibers can be arranged for the desired content of reinforcements. The lay-up is encased in a metal can which is sealed and evacuated. The whole assembly is subsequently heated and pressed to facilitate the development of diffusion bonding. The applied pressure and temperature, as well as their duration's for diffusion bonding to develop, vary with the composite systems. For instance, the boron -aluminum composite develops satisfactory bonding at 454°C under a pressure of 4.14×10^7 N/m² has been observed for 6061 Al reinforced with 48 volume per cent of boron fibers by diffusion bonding. Prolonged hot

pressing may cause reduction in the composite strength. The change of microstructure accompanying the reduction in strength in figure below for a stainless steel-aluminum composite material. This composite contains 27 percent stain-less steel.

The formation of an inter-metallic compound in the vicinity of the fiber-matrix interface is responsible for the weakening of the composite strength. The diffusion bonding process may also be used to consolidate tape forms produced by methods such as plasma spray, hot rolling, and vapor deposition. The tapes easy to handle and can be arranged in predetermined orientations .

d) Electroforming

Electroforming has the advantage of combining the fiber and matrix materials at low temperatures, and thus degradation of reinforcing materials can be avoided. The major apparatuses for electroforming consist of a plating bath a mandrel which serves as the cathode in the deposition process. A continuous filament is wound onto the mandrel while the metal matrix material is being deposited. The spacing filaments can be closely controlled in the winding process, and high-volume fractions of fiber content can be achieved. Monolayer tapes formed by process can be further consolidated into composite structure members by diffusion bonding. For multilayer composites formed in this manner, voids tend to form between fibers and between successively deposited layers. Filaments of boron, silicon carbide, and tungsten have been successively incorporated into a nickel matrix by electroforming. Other matrix metals, as well as alumina whiskers, also have been employed in this method of fabrication.

e) Vapor Deposition

The process of vapor deposition is carried out by decomposing a compound of metal matrix material and its subsequent deposition on the reinforcing materials. The reinforcements can be in the forms of continuous filaments or random whisker mats. A main advantage of this technique is that the chemical decomposition process can be accomplished at a relatively low temperature and the degradation of fibers can be minimized. High-volume fraction of fiber can be attained by this process. However, the slow

and costly process of vapor deposition is its major disadvantage. Metals such as aluminum and nickel have been used for deposition.

f) Rolling

Both hot and cold rolling can be employed to incorporate filaments and metal strips into continuous tapes. In this processes, the fibers and metal strips are fed through rollers under applied pressure. The rollers are heated to a high temperature in the case of hot-rolling. Both pressure and temperature serve to accelerate diffusion bonding, although the contact time of the composite assembly with the applied pressure and temperature is relatively short. The metal strips can be grooved in order to provide precise alignment of the filaments. The sandwich construction of continuous tapes by the rolling process is restricted to a few layers in thickness. However, tapes fabricated in this manner can be laid up and further consolidated by diffusion bonding. The rolling process can also be used to consolidate continuous fibers coated with a metallic matrix material.

g) Extrusion

One method of extrusion is known as co-extrusion, which does not need the application of high temperature. Figure 3. 4 below indicates a design of extrusion tooling for making composite wires. The wire, consisting of a steels core surrounded by an aluminum alloy sheath, is produced by simultaneous feeding of the reinforcing filament and extruding of the matrix metal. Composite wires formed in this manner can be further rolled into tapes plates through diffusion bonding. There are other methods of extrusion in which fibers are first aligned in matrix powders, and this assembly is pressed into the form of bars. A single perform, or several of them sealed in can, are then extruded to the desired dimension.

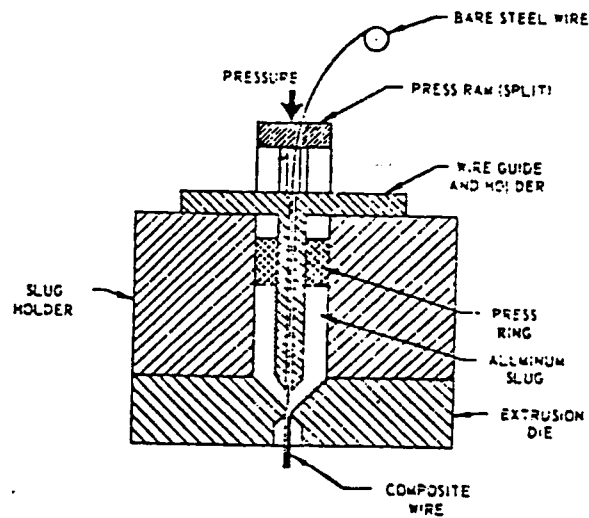


Figure 3. 4 Design of extrusion tooling

h) Other Methods

Methods including plasma spray, pneumatic impaction, and the simultaneous growth of the reinforcing and matrix materials from a melt also have been used for producing metal-matrix composites. The method of plasma spray is suitable for low melting point metals. It employs a plasma torch which sprays matrix materials in the form of liquid droplets on to rotating mandrel covered with aligned fibers. The composite formed is then removed from the mandrel and hot-pressed to eliminate voids. As one example, aluminum has been successively sprayed on silicone carbide-coated boron fiber. Composite tapes formed in this manner can be further consolidated into structural parts by diffusion bonding. Pneumatic impaction has been used to consolidate the mixture of metal powders and reinforcing materials by applying high pressure impact. In view of its basic difference in the fabrication process relative to all the other methods.

An examination of the fabrication methods reviewed above indicates that the matrix used in the consolidation process may assume different forms. These include the metallic powders used in pneumatic impaction and the powder metallurgy technique; the liquid form used in liquid metal infiltration and plasma spray; the molecular form of matrix metals appearing in the electroforming and vapor deposition processes; and the metal foils employed in diffusion bonding and the rolling process. It is also noted that one form of matrix metal incorporated with reinforcements may be subjected to more than one fabrication process. For instance, composite materials produced by sintering are

subsequently extruded and rolled. Monolayer tapes fabricated by various methods may also be further consolidated by rolling and diffusion bonding.

3.7 Properties of Aluminum-Stainless-Steel Composites

Metallic materials have been reinforced with all kinds of fiber materials discussed before. Now we represent Aluminum-Stainless-steel composite which is manufactured by this thesis. In this process the diffusion bonding method is used.

First, aluminum foils layered up in a mold then stainless-steel wires put it up. This layer is done replace three times. This layers are put in a mold. The mold is heated until 550°C then pressed at 24.66 Mpa during 15 minutes. At the end of pressing, mold is cooled at room temperature. After this process we start examining the composite. These tests are made :

3.7.1 Tensile Test In Elastic Region

This test is made only elastic region. A tensile specimen is prepared 2-direction (at 90° angle with reinforced direction). And pasted one strain-gage only. This gage is measured elongation of tensile direction. Thus, we obtain Modulus of Elasticity of material (E_2). After this test we prepare a tensile test specimen that is at 45° angle with reinforced direction. Thus, we obtain Shearing Modulus of material (G_{12}) by calculation.

After these processes we obtain ultimate tensile strength and shearing strength of material (X , Y , S). Table below indicates these properties.

3.7.2 Tensile Test In Elastic And Plastic Region

This test is made two steps. First 1-direction (reinforced direction) tensile test is made in elastic region. We prepared a tensile test specimen that 0° angle with reinforce direction two stain-gages pasted to it. One of them measured elongation that tensile direction other measured 90° angle with tensile direction. Thus we obtain Modulus of Elasticity of material (E_1), Poisson's ratio (ν_{12}). After this loading tensile load is increased up to failure. Thus, we obtain plastic material properties (K , n).

3.8 Stress - Strain Relations for Plane Stress in an Orthotropic Material

Three dimensional stress - strain relations in an orthotropic material can be written as :

$$\begin{Bmatrix} \sigma_1 \\ \sigma_2 \\ \sigma_3 \\ \tau_{23} \\ \tau_{31} \\ \tau_{12} \end{Bmatrix} = \begin{bmatrix} C_{11} & C_{12} & C_{13} & 0 & 0 & 0 \\ C_{21} & C_{22} & C_{23} & 0 & 0 & 0 \\ C_{31} & C_{32} & C_{33} & 0 & 0 & 0 \\ 0 & 0 & 0 & C_{44} & 0 & 0 \\ 0 & 0 & 0 & 0 & C_{55} & 0 \\ 0 & 0 & 0 & 0 & 0 & C_{66} \end{bmatrix} \begin{Bmatrix} \varepsilon_1 \\ \varepsilon_2 \\ \varepsilon_3 \\ \gamma_{23} \\ \gamma_{31} \\ \gamma_{12} \end{Bmatrix} \quad (3.1)$$

For orthotropic material, the strain - stress relations can also be written in the following form :

$$\begin{Bmatrix} \varepsilon_1 \\ \varepsilon_2 \\ \varepsilon_3 \\ \gamma_{23} \\ \gamma_{31} \\ \gamma_{12} \end{Bmatrix} = \begin{bmatrix} S_{11} & S_{12} & S_{13} & 0 & 0 & 0 \\ S_{21} & S_{22} & S_{23} & 0 & 0 & 0 \\ S_{31} & S_{32} & S_{33} & 0 & 0 & 0 \\ 0 & 0 & 0 & S_{44} & 0 & 0 \\ 0 & 0 & 0 & 0 & S_{55} & 0 \\ 0 & 0 & 0 & 0 & 0 & S_{66} \end{bmatrix} \begin{Bmatrix} \sigma_1 \\ \sigma_2 \\ \sigma_3 \\ \tau_{23} \\ \tau_{31} \\ \tau_{12} \end{Bmatrix} \quad (3.2)$$

For a lamina in the 1-2 plane as shown in Figure 3. 5, a plane stress state is defined by setting

$$\sigma_3 = \tau_{23} = \tau_{31} = 0 \quad (3.3)$$

in the three dimensional stress - strain relations given in Equation 3. 1. For orthotropic material, such a procedure results in implied strains of

$$\begin{aligned} \varepsilon_3 &= S_{13} \sigma_1 + S_{23} \sigma_2 \\ \gamma_{23} &= \gamma_{31} = 0 \end{aligned} \quad (3.4)$$

Moreover, the strain - stress relations in Equation 3. 2 reduce to

$$\begin{Bmatrix} \varepsilon_1 \\ \varepsilon_2 \\ \gamma_{12} \end{Bmatrix} = \begin{bmatrix} S_{11} & S_{12} & 0 \\ S_{12} & S_{22} & 0 \\ 0 & 0 & S_{66} \end{bmatrix} \begin{Bmatrix} \sigma_1 \\ \sigma_2 \\ \tau_{12} \end{Bmatrix} \quad (3.5)$$

where

$$\begin{aligned} S_{11} &= \frac{1}{E_1}, & S_{12} &= -\frac{\nu_{12}}{E_1} = -\frac{\nu_{21}}{E_2} \\ S_{22} &= \frac{1}{E_2}, & S_{66} &= \frac{1}{G_{12}} \end{aligned} \quad (3.6)$$

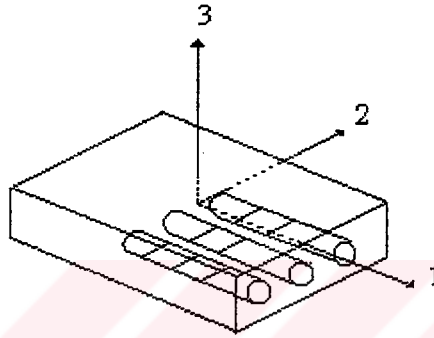


Figure 3. 5 Unidirectionally reinforced lamina

The strain - stress relations in Equation 3. 5 can be inverted to obtain the stress-strain relations:

$$\begin{Bmatrix} \sigma_1 \\ \sigma_2 \\ \tau_{12} \end{Bmatrix} = \begin{bmatrix} C_{11} & C_{12} & 0 \\ C_{12} & C_{22} & 0 \\ 0 & 0 & C_{66} \end{bmatrix} \begin{Bmatrix} \varepsilon_1 \\ \varepsilon_2 \\ \gamma_{12} \end{Bmatrix} \quad (3.7)$$

where

$$\begin{aligned} C_{11} &= \frac{S_{22}}{S_{11} \cdot S_{22} - S_{12}^2}, & C_{12} &= \frac{S_{12}}{S_{11} \cdot S_{22} - S_{12}^2} \\ C_{22} &= \frac{S_{11}}{S_{11} \cdot S_{22} - S_{12}^2}, & C_{66} &= \frac{1}{S_{66}} \end{aligned} \quad (3.8)$$

or, in terms of the engineering constant,

$$\begin{aligned}
C_{11} &= \frac{E_{11}}{1 - \nu_{12} \cdot \nu_{21}} \quad , \quad C_{12} = \frac{\nu_{12} \cdot E_2}{1 - \nu_{12} \cdot \nu_{21}} = \frac{\nu_{21} \cdot E_1}{1 - \nu_{12} \cdot \nu_{21}} \\
C_{22} &= \frac{E_2}{1 - \nu_{12} \cdot \nu_{21}} \quad , \quad C_{66} = G_{12}
\end{aligned}
\tag{3.9}$$

Note that there are four independent material properties, E_1 , E_2 , G_{12} , ν_{12}

3.9 Experimental Determination of Strength and Stiffness

For orthotropic materials with equal properties in tension and compression, certain basic experiments can be performed to obtain the properties in the principal material directions. The experiments, if conducted properly, generally reveal both the strength and stiffness characteristics of the material. The stiffness characteristics are

E_1 = Young's modulus in the 1-direction

E_2 = Young's modulus in the 2-direction

G_{12} = Shear modulus in the 1-2 plane

$\nu_{12} = -\epsilon_2 / \epsilon_1$ for $\sigma_1 = \sigma$ and all other stresses are zero

$\nu_{21} = -\epsilon_1 / \epsilon_2$ for $\sigma_2 = \sigma$ and all other stresses are zero

where only three of E_1 , E_2 and ν_{21} are independent and the strength characteristics are

X = axial or longitudinal strength (1- direction)

Y = transverse strength (2- direction)

S = Shear strength (1-2 plane)

Several experiments will now be described from which the foregoing basic tenet of the experiments is that the stress- strain behavior of the materials is linear from zero load to the ultimate or fracture load. Such linear behavior is typical for glass/epoxy composites and is quite reasonable for boron/epoxy composites except for the shear behavior which is nonlinear to fracture. This characteristics of the linear elastic behavior to fracture is quite similar to the analysis bodies that exhibit linear elastic behavior up until the onset plastic. Thus, certain concepts of the theory of plasticity such as yield functions are useful analogues for the strength theories that will be discussed later.

First consider a uniaxial tension test in the 1- direction on a flat piece of unidirectionally reinforced lamina as shown in Figure 3. 6. The strain ε_1 and ε_2 are measured in the test whereupon, by definition,,

$$\begin{aligned} \sigma_1 &= \frac{P}{A} & , & & E_1 &= \frac{\sigma_1}{\varepsilon_1} \\ \vartheta_{12} &= -\frac{\varepsilon_2}{\varepsilon_1} & , & & X &= \frac{P_{\text{ult}}}{A} \end{aligned} \quad (3.10)$$

where A is the cross-sectional area of the specimen and perpendicular to the applied load.

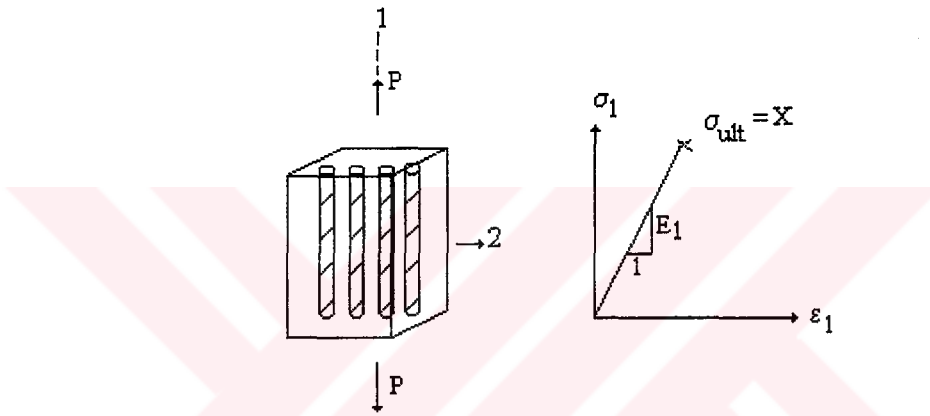


Figure 3. 6 Uniaxially loading in the 1-direction

Second, consider a uniaxial tension test in the 2-direction on a flat piece of unidirectionally reinforced lamina as in Figure 3. 7. As in the first experiment, ε_1 and ε_2 are measured so

$$\begin{aligned} \sigma_2 &= \frac{P}{A} & , & & E_2 &= \frac{\sigma_2}{\varepsilon_2} \\ \vartheta_{21} &= -\frac{\varepsilon_1}{\varepsilon_2} & , & & Y &= \frac{P_{\text{ult}}}{A} \end{aligned} \quad (3.11)$$

where again A is the cross-sectional area of the specimen end. At this point, stiffness properties satisfy the reciprocal relations

$$\frac{\vartheta_{12}}{E_1} = \frac{\vartheta_{21}}{E_2} \quad (3.12)$$

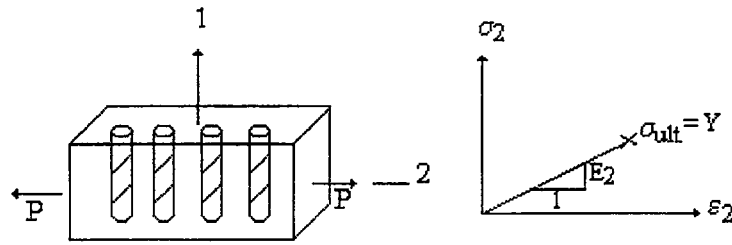


Figure 3. 7 Uniaxial loading in the 2-direction

Third, consider a uniaxial tension test at 45° to the 1-direction on a flat piece of the lamina as shown in Figure 3. 8. By measurement of ϵ_x alone, obviously

$$E_x = \frac{P/A}{\epsilon_x} \quad (3.13)$$

Engineering constant E_x for orthotropic lamina that is stressed in nonprinciple xy coordinates are

$$\frac{1}{E_x} = \frac{1}{E_1} \cos^4 \theta + \left(\frac{1}{G_{12}} - \frac{2\nu_{12}}{E_1} \right) \sin^2 \theta \cos^2 \theta + \frac{1}{E_2} \sin^4 \theta \quad (3.14)$$

Then, by use of the transformation relations in Equation 3. 12

$$\frac{1}{E_x} = \frac{1}{4} \left(\frac{1}{E_1} - \frac{2\nu_{12}}{E_1} + \frac{1}{G_{12}} + \frac{1}{E_2} \right) \quad (3.15)$$

wherein G_{12} is the only unknown. Thus,

$$\frac{1}{G_{12}} = \frac{4}{E_x} - \frac{1}{E_1} - \frac{1}{E_2} + \frac{2\nu_{12}}{E_1} \quad (3.16)$$

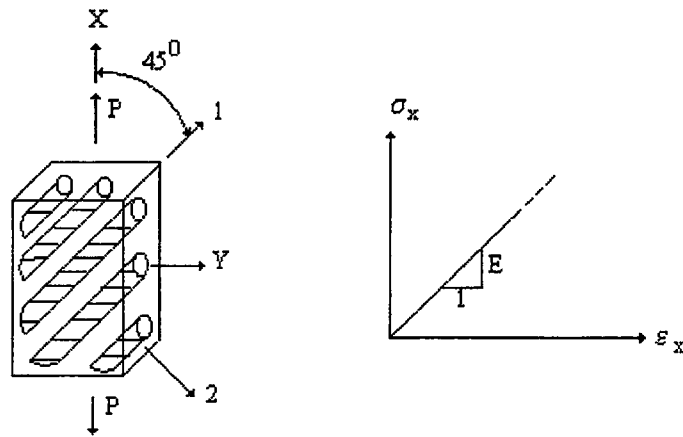


Figure 3. 8 Uniaxial loading at 45° to the 1- direction

3.10 Biaxial Strength Theories For An Orthotropic Lamina

Our attention in this section will be restricted to biaxial loading. Some of the biaxial strength theories that have been studied are:

1. Maximum stress theory
2. Maximum strain theory
3. Tsai-hill theory
4. Tsai-Wu tensor theory

3.10.1 Maximum Stress Theory

In the maximum stress theory, the stresses in principal material directions must be less than the respective strengths, otherwise fracture is said to have occurred that is, for tensile stresses,

$$\begin{aligned}
 \sigma_1 &< X_t \\
 \sigma_2 &< Y_t \\
 \tau_{12} &< S
 \end{aligned}
 \tag{3.17}$$

and for compressive stresses

$$\begin{aligned}\sigma_1 &> X_c \\ \sigma_2 &> Y_t\end{aligned}\quad (3.18)$$

Note that the shear strength is independent of the sign of τ_{12} . If any one of the foregoing inequalities is not satisfied, then the assumption is made that the material has failed by the failure mechanism associated with X_t , X_c , Y_t , Y_c , or S , respectively. Note that there is *no* interaction between modes of failure in this criterion - there are actually three subcriteria.

In applications of the maximum stress criterion, the stresses in the body under consideration must be transformed to stresses in the principal material directions. For example, Tsai considered a unidirectional reinforced composite subjected to uniaxial load at angle θ to the fibers.

$$\begin{aligned}\sigma_1 &= \sigma_x \cos^2 \theta \\ \sigma_2 &= \sigma_x \sin^2 \theta \\ \tau_{12} &= -\sigma_x \sin \theta \cos \theta\end{aligned}\quad (3.19)$$

Then by inversion of Equation 3.19 and substitution of Equation 3.17 the maximum uniaxial stress, σ_x , is the smallest of

$$\begin{aligned}\sigma_x &< \frac{X}{\cos^2 \theta} \\ \sigma_x &< \frac{Y}{\sin^2 \theta} \\ \sigma_x &< \frac{S}{\sin \theta \cos \theta}\end{aligned}\quad (3.20)$$

3.10.2 Maximum Strain Theory

The maximum strain theory is quite similar to the maximum stress theory. Here, strains are limited rather than stresses. Specifically, the material is said to have failed if one or more of the following inequalities is not satisfied :

$$\begin{aligned}
 \sigma_1 &< X_t \\
 \sigma_2 &< Y_t \\
 |\tau_{12}| &< S
 \end{aligned}
 \tag{3.21}$$

Includes for materials with different strength in tension and compression

$$\begin{aligned}
 \sigma_1 &> X_c \\
 \sigma_2 &> Y_t
 \end{aligned}
 \tag{3.22}$$

where

X_{tc} , X_{cc} are maximum tensile and compressive normal strain in the 1-direction
 Y_{tc} , Y_{cc} are maximum tensile and compressive normal strain in the 2-direction
 S_s is maximum shear strain in the 1-2 plane

As with shear strength, the maximum shear strain is unaffected by the sign of the shear stress. The strains in principal material directions, ϵ_1 , ϵ_2 , γ_{12} , must be found from the strains in body coordinates by transformation before the criterion can be applied.

For a unidirectional reinforced composite subjected to uniaxial load at angle θ to the fibers (the example of problem in the section on maximum stress theory) the allowable stresses can be found from the allowable strains X_{tc} , Y_{tc} , etc. in the following manner.

First given that the stress-strain relations are

$$\begin{aligned}
 \epsilon_1 &= \frac{1}{E_1} \cdot (\sigma_1 - \nu_{12} \cdot \sigma_2) \\
 \epsilon_2 &= \frac{1}{E_2} \cdot (\sigma_2 - \nu_{21} \cdot \sigma_1) \\
 \gamma_{12} &= \frac{\tau_{12}}{G_{12}}
 \end{aligned}
 \tag{3.23}$$

upon substitution of the transformation equations

$$\begin{aligned}
\sigma_1 &= \sigma_x \cos^2 \theta \\
\sigma_2 &= \sigma_x \sin^2 \theta \\
\tau_{12} &= -\sigma_x \sin \theta \cos \theta
\end{aligned}
\tag{3.24}$$

In the stress-strain relations Equation 3. 23 the strains can be expressed as

$$\begin{aligned}
\varepsilon_1 &= \frac{1}{E_1} \cdot (\cos^2 \theta - \nu_{12} \cdot \sin^2 \theta) \cdot \sigma_x \\
\varepsilon_2 &= \frac{1}{E_2} \cdot (\sin^2 \theta - \nu_{21} \cdot \cos^2 \theta) \cdot \sigma_x \\
\gamma_{12} &= \frac{1}{G_{12}} \cdot (\sin \theta \cdot \cos \theta) \cdot \sigma_x
\end{aligned}
\tag{3.25}$$

Finally, if the usual restriction to linear elastic behavior to the failure is made,

$$\begin{aligned}
X_{et} &= \frac{X_t}{E_1} \\
Y_{et} &= \frac{Y_t}{E_2} \\
S_\varepsilon &= \frac{S}{G_{12}}
\end{aligned}
\tag{3.26}$$

and

$$\begin{aligned}
X_{\varepsilon c} &= \frac{X_c}{E_1} \\
Y_{\varepsilon c} &= \frac{Y_c}{E_2}
\end{aligned}
\tag{3.27}$$

(which could equally well come from measured values in an experiment), then the maximum strain criterion for this example can be expressed as

$$\begin{aligned}
\sigma_x &< \frac{X}{\cos^2 \theta - \nu_{12} \cdot \sin^2 \theta} \\
\sigma_x &< \frac{Y}{\sin^2 \theta - \nu_{21} \cos^2 \theta} \\
\sigma_x &< \frac{S}{\sin \theta \cdot \cos \theta}
\end{aligned}
\tag{3.28}$$

By comparison of the maximum strain criterion Equation 3. 20 with the maximum stress criterion Equation 3. 21, it is obvious that the only difference is the inclusion of Poisson's ratio terms in the strain criterion.

3.10.3 Tsai-Hill Theory

Hill proposed a yield criterion for anisotropic materials :

$$(G+H) \sigma_1^2 + (F+H) \sigma_2^2 + (F+G) \sigma_3^2 - 2H\sigma_1\sigma_2 - 2G\sigma_1\sigma_3 - 2F\sigma_3\sigma_2 + 2L\tau_{23}^2 + 2M\tau_{13}^2 + 2N\tau_{12}^2 = 1 \quad (3.29)$$

This anisotropic yield criterion will be used as an isotropic strength criterion in the spirit of both being limits of linear elastic behavior. Thus, Hill's yield strengths F, G, H, L, M, and N will be regarded as failure strengths. Hill's theory is an extension of von-Mises' isotropic yield criterion. The von-Mises criterion, in turn, can be related to the amount of energy that is used to distort the body rather than to change its volume. However, distortion cannot be separated from dilatation in orthotropic materials so Equation 3.29 is not related to distortional energy failure theory.

The failure strength parameters F, G, H, L, M, and N were related to the usual failure strengths X, Y, and S for a lamina by Tsai. First, if only τ_{12} acts on the body then, since its maximum value is S;

$$2N = \frac{1}{S^2} \quad (3.30)$$

Similarly, if only σ_1 acts on the body, then

$$G + H = \frac{1}{X^2} \quad (3.31)$$

and if only σ_2 acts, then

$$F + H = \frac{1}{Y^2} \quad (3.32)$$

the strength in the 3-direction is denoted by Z and only σ_3 acts, then

$$F + G = \frac{1}{Z^2}$$

$$2H = \frac{1}{X^2} + \frac{1}{Y^2} - \frac{1}{Z^2}$$

$$2G = \frac{1}{X^2} + \frac{1}{Z^2} - \frac{1}{Y^2}$$

$$2F = \frac{1}{Y^2} + \frac{1}{Z^2} - \frac{1}{X^2}$$

(3. 33)

For plane stress in the 1-2 plane of a unidirectional lamina with fibers in the 1-direction, $\sigma_3 = \tau_{13} = \tau_{23} = 0$. However, from the cross section of such a lamina in Figure 3. 9., $Y = Z$ from geometrical symmetry considerations. Thus, Equation 3. 29 leads to

$$\frac{\sigma_1^2}{X^2} - \frac{\sigma_1 \sigma_2}{X^2} + \frac{\sigma_2^2}{Y^2} + \frac{\tau_{12}^2}{S^2} = 1$$

(3. 34)

as the governing failure criterion in terms of the familiar lamina strengths X, Y, and S.

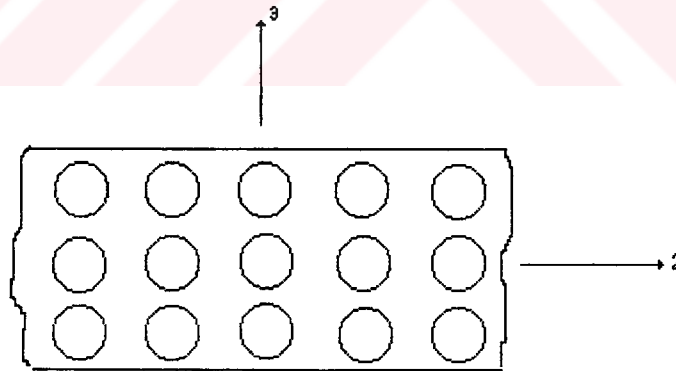


Figure 3. 9 Cross section of unidirectional lamina with fibers in the 1-direction

Finally, for the off-axis composite example, substitution of the Equation 3. 24 (stress transformation equations) in Equation 3. 35 yields the Tsai-Hill failure criterion

$$\frac{\cos^4 \theta}{X^2} + \left(\frac{1}{S^2} - \frac{1}{X^2} \right) \cos^2 \theta \sin^2 \theta + \frac{\sin^4 \theta}{Y^2} = \frac{1}{\sigma_x^2}$$

(3. 35)

3.10.4 Tsai-Wu Tensor Theory

The preceding biaxial strength theories suffer from various inadequacies in their description of experimental data. One obvious way to improve the correlation between theory and experiment is to increase the number of terms in the prediction equation. This increase in curve fitting ability plus the added feature of representing the various strengths in tensor form was used by Tsai and Wu. In the processes, several new strength definitions are required, mainly having to do with interaction between stresses in two directions.

Tsai and Wu postulated that a failure surface in stress space exists in the form

$$F_i\sigma_i + F_{ij}\sigma_i\sigma_j = 1 \quad i, j = 1, 2, \dots, 6 \quad (3.36)$$

Where in F_i and F_{ij} are strength tensors of the second and fourth rank, respectively and the usual contracted stress notation is used except that $\sigma_4 = \tau_{23}$, $\sigma_5 = \tau_{31}$, $\sigma_6 = \tau_{12}$. Equation 3.36 is obviously very complicated; we will restrict our attention to the reduction of Equation 3.36 for an orthotropic lamina under plane stress conditions :

$$F_1\sigma_1 + F_2\sigma_2 + F_4\sigma_4 + F_{11}\sigma_1^2 + F_{22}\sigma_2^2 + F_{44}\sigma_4^2 + 2F_{12}\sigma_1\sigma_2 = 1 \quad (3.37)$$

The terms that are linear in the stresses are useful in representing different strengths in tension and compression. The terms that are quadratic in the stresses are the more or less usual terms to represent an ellipsoid in stress space. However, the term involving F_{12} is entirely new to us and is used to represent the interaction between normal stresses in the 1- and 2- directions in a manner quite unlike the shear strength.

Some of the components of the strength tensors are defined in terms of the engineering strengths already discussed. For example, consider a uniaxial load on a specimen in the 1- direction. Under tensile load, the engineering strength is X_t whereas under compressive load, it is X_c . Thus under tensile load,

$$F_1X_t + F_{11}X_t^2 = 1 \quad (3.38)$$

and under compressive load,

$$F_1 X_c + F_{11} X_c^2 = 1 \quad (3.39)$$

Upon simultaneous solution of Equations 3.39 and 3.40

$$\begin{aligned} F_1 &= \frac{1}{X_t} + \frac{1}{X_c} \\ F_{11} &= -\frac{1}{X_t X_c} \end{aligned} \quad (3.40)$$

Similarly ,

$$\begin{aligned} F_2 &= \frac{1}{Y_t} + \frac{1}{Y_c} \\ F_{22} &= -\frac{1}{Y_t Y_c} \end{aligned} \quad (3.41)$$

and

$$\begin{aligned} F_6 &= 0 \\ F_{66} &= \frac{1}{S^2} \end{aligned} \quad (3.42)$$

The determination of the fourth rank tensor term F_{12} remains. Basically, F_{12} cannot be determined from any uniaxial test in the principal material directions. Instead, biaxial test must be used. This fact should be surprising since F_{12} is the coefficient of σ_1 and σ_2 in the failure criterion, Equation 3.38. Thus, for example, we can impose a state of biaxial tension described by $\sigma_1 = \sigma_2 = \sigma$ and all stresses are zero. Accordingly, from Equation 3.38.

$$(F_1 + F_2) \sigma + (F_{11} + F_{22} + 2F_{12}) \sigma^2 = 1 \quad (3.43)$$

Now solve for F_{12} after substituting the definitions just derived for F_1 , F_2 , F_{11} , and F_{22} :

$$F_{12} = \frac{1}{2\sigma^2} \left(1 - \left(\frac{1}{X_t} + \frac{1}{X_c} + \frac{1}{Y_t} + \frac{1}{Y_c} \right) \sigma + \left(\frac{1}{X_t X_c} + \frac{1}{Y_t Y_c} \right) \sigma^2 \right) \quad (3.44)$$

The value of F_{12} then depends on the various engineering strengths plus the biaxial tensile failure stress, σ . Tsai and Wu also discuss the use of off-axis uniaxial tests to determine the interaction strengths such as F_{12} .

At this point recall that all interaction between normal stresses σ_1 and σ_2 in the Tsai-Hill theory is related to the strength in the 1-direction :

$$\frac{\sigma_1^2}{X^2} - \frac{\sigma_1\sigma_2}{X^2} + \frac{\sigma_2^2}{Y^2} + \frac{\tau_{12}^2}{S^2} = 1 \quad (3.45)$$

The Tsai-Hill tensor failure theory is obviously of more general character than Tsai-Hill theory. Specific advantages of Tsai-Wu theory include :

1. Invariance under rotation or redefinition of coordinates,
2. Transformation via known tensor transformation laws,
3. Symmetry properties akin to those of the stiffness and compliance's.

Accordingly, the mathematical operations with this tensor failure theory are well known and relatively straightforward.

3.11 Elasto- Plastic Analysis of Orthotropic Composite Materials

In the Orthotropic materials, the procedure of the elasto-plastic analysis is same as isotropic materials, only the yield criterion changes.

Defining the plastic potential, or effective stress, $\bar{\sigma}$, in a similar manner to the Huber-Mises yield function for isotropic material, we can write for plane stress condition

$$\bar{\sigma}^2 = a_1 \cdot \sigma_1^2 + 2 \cdot a_{12} \cdot \sigma_1 \cdot \sigma_2 + a_2 \cdot \sigma_2^2 + a_6 \cdot \tau_{12}^2 \quad (3.46)$$

where σ_1 , σ_2 , and τ_{12} are the non-zero stress components and a_1 , a_2 , a_{12} and a_6 are anisotropic parameters which can be determined experimentally.

In matrix form, this yield function can be written as

$$\bar{\sigma}^2 = \{\sigma\}^T \cdot [A] \cdot \{\sigma\} \quad (3.47)$$

where

$$\{\sigma\} = \{\sigma_1, \sigma_2, \tau_{12}\}^T \quad (3.48)$$

and

$$[A] = \begin{bmatrix} a_1 & a_{12} & 0 \\ a_{12} & a_2 & 0 \\ 0 & 0 & a_6 \end{bmatrix} \quad (3.49)$$

These parameters can be determined by four independent yield test. For a tensile test in the 1-direction, we have

$$a_1 = \frac{\sigma_1^2}{\sigma_1^2} \quad (3.50)$$

Taking the 1-direction as the reference direction, $\bar{\sigma} = \sigma_1 = X$, then $a_1 = 1$. Similarly

$$a_{12} = -\frac{1}{2}, \quad a_2 = \frac{X^2}{Y^2}, \quad a_6 = \frac{X^2}{S^2}, \quad (3.51)$$

and substituting these parameters into Equation 3. 46, we obtain Tsai-Hill theory. We can write Equation 3. 32 following form

$$\bar{\sigma} = X = \left[\sigma_1^2 - \sigma_1 \cdot \sigma_2 + \frac{X^2}{Y^2} \cdot \sigma_2^2 + \frac{X^2}{S^2} \cdot \tau_{12}^2 \right]^{1/2} \quad (3.52)$$

If the effective stress $\bar{\sigma}$, is greater than yield stress σ_y , elasto-plastic analysis are made like isotropic materials.

CHAPTER FOUR

DEFINITION AND FORMULATION

4.1. Definition of The Problem

The geometry of plate is shown in Figure 4. 1. In this application, The plates are loaded in various uniaxial tension and used orientation angles are 0° , 30° , 45° , 60° and 90° . These loads are 70, 75, 80 MPa for 0° , 45, 50, 55 MPa for 30° , 30, 35, 40 MPa for 45° , 20, 25, 30 MPa for 60° and 15, 20, 25 MPa for 90° .

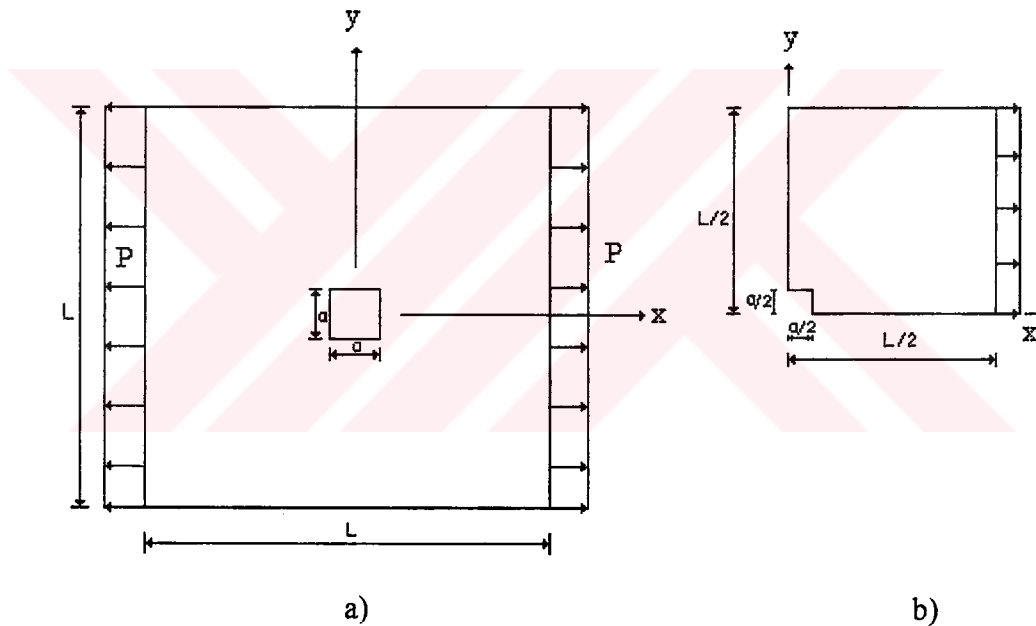


Figure 4. 1 a) Whole square plate, b) a quarter plate

In the 0° and 90° angles because of symmetry with respect to x and y axis of shape, loading and material properties a quarter of the plate is taken finite element model. In the other angles, whole plate is used as finite element model.

The plates with a square hole are symbolically divided into finite elements as shown in Figure 4. 2. These square holes are 20, 40 and 60mm.

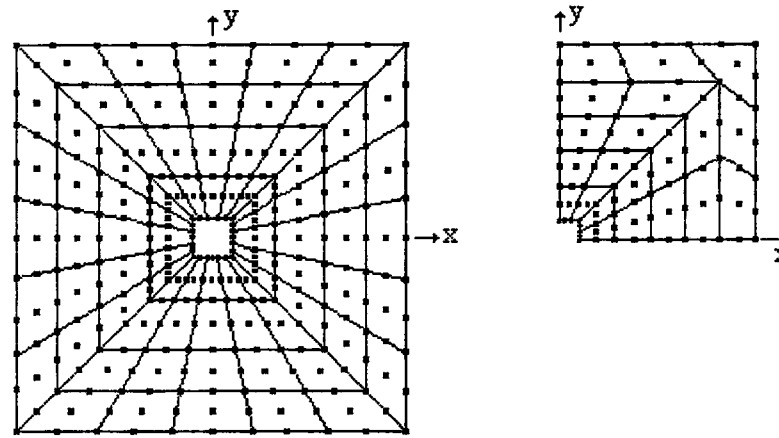


Figure 4.2 Mesh Generation Whole and 1/4 plate

In the solution of the problem, two dimensional isoparametric rectangular element with nine nodes is used. The finite element model consist of 80 meshes and 360 nodal points.

4.2. Formulation of The Finite Element

By using finite elements formulation following equation

$$\{F\} = [K].\{\delta\} \quad (4.1)$$

derivated. Where $\{F\}$ external force, $[K]$ stiffness matrix and $\{\delta\}$ displacement vector of system. For a given set of prescribed boundary condition and external forces acting on the body Equation 4. 1 can be solved uniquely for the nodal displacement $\{\delta\}$, from which the stresses and strains within the body can subsequently be computed. And by using Tsai-Hill flow criteria the equivalent stresses are can be calculated. The results are compared to residual stresses and the equivalent stresses are determined. The nodals which are stated into plastic region are found by comparing the results which residual stresses. Finally, with the initial stress method the elasto-plastic stress analysis has been done.

CHAPTER FIVE

RESULTS AND CONCLUSIONS

1. Results and Conclusions

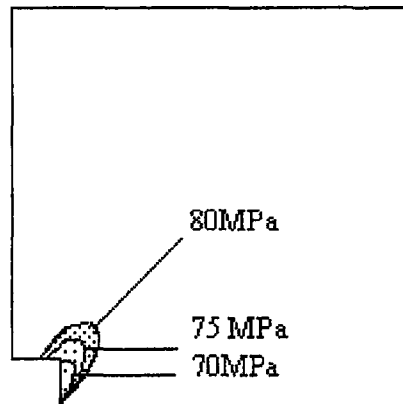
In this study, orientation of plastic regions and internal stresses for uniform tension loads of various square holes are shown. Stresses, which are caused by linear elastic events, are marked with opposite sign according to stresses which are composed within plastic regions after external forces are removed. So, in the condition of application of tension loads when after internal stresses has been occurred, the stresses that neighbour to notch reduces the newest stresses and reduces the concentration of stresses that also neighbour to notch. Therefore, the plastic region becomes noncritical region. In this state, the critical region is the boundary region, because of the small amount of stress concentration the plate subject to more amount of loading according to the elastically plates loaded plates. By the way, the plate has more strength to higher amount of loads within using high strength materials.

If the compressive loads are applied after the formation of internal stresses, the stresses becomes dangerous due to internal and compressive load stresses have the same sign effect. As a result, if plate subjected to tension loads, the internal stresses should be existed by tension loads and in the situation of compressive loading the internal stresses should be existed by compressive loads.

The following figures are draw by means of prepared computer program. From page 50 to 57, the yielding points are pointed out and the area which contains these yielding points stayed in the plastic region. In the Figures 5. 1, and 5. 2, because of symmetry, the figures show plastic regions on a quarter plate. In the Figures 5. 3 to 5. 5 the whole plate plastic region separation are shown. In addition, in the other figures residual stresses which are occurred in a quarter plate only in the x axis which is lied along upper points of the hole and the diagonal from last point of the x axis to the last point of the corner are shown

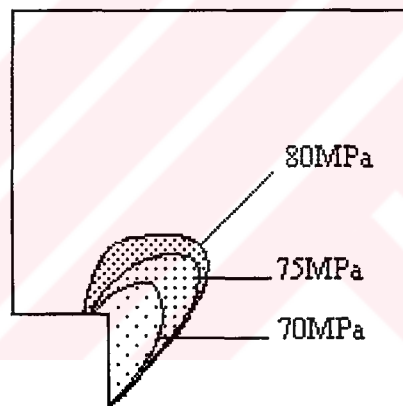
graphically. By the same way, the residual stresses for a whole plate are shown graphically.

$a=20\text{ mm}$



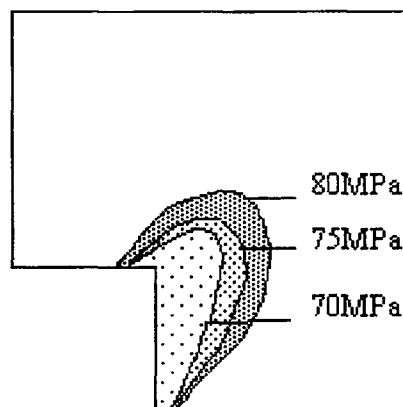
a)

$a=40\text{ mm}$



b)

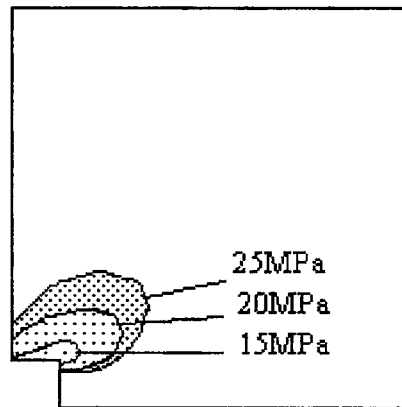
$a=60\text{ mm}$



c)

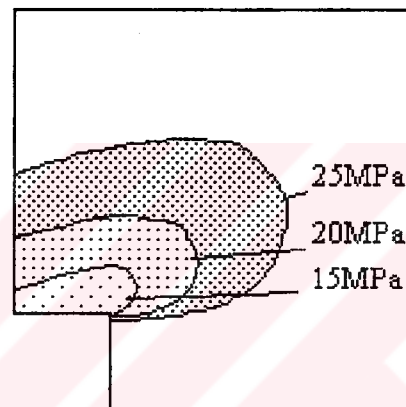
Figure 5. 1 $\theta = 0^\circ$, Plastic regions on quarter plates, a) hole size 20x20mm b) hole size 40x40mm and c) hole size 60x60mm

$a=20\text{mm}$



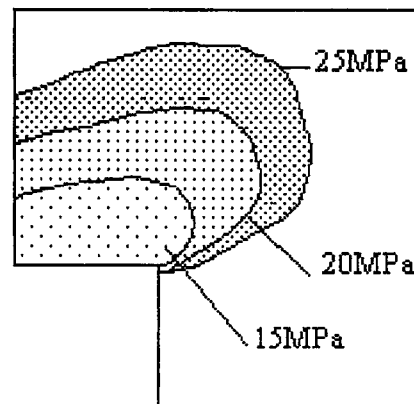
a)

$a=40\text{mm}$



b)

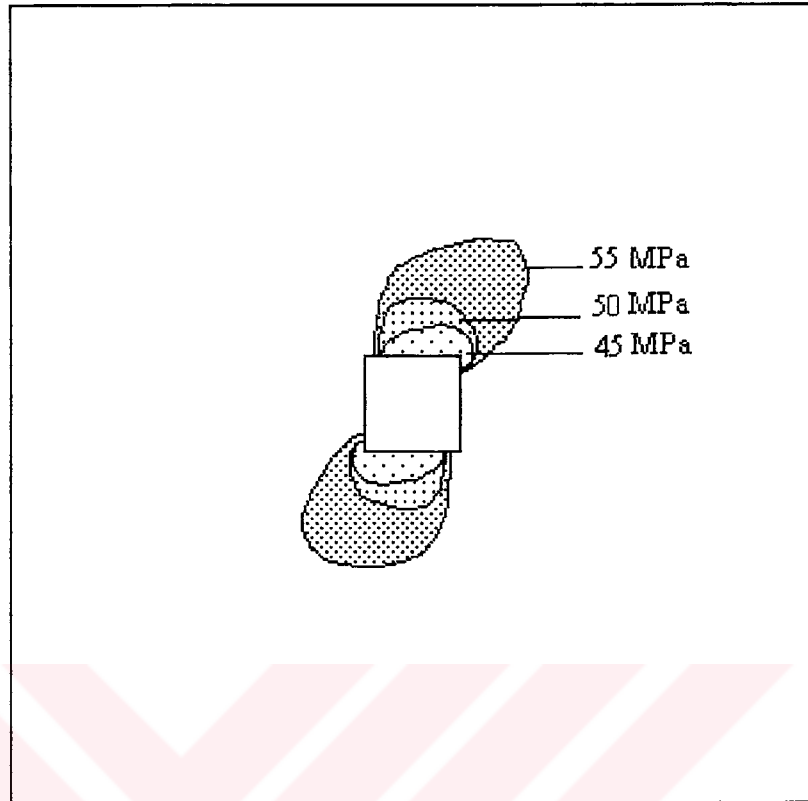
$a=60\text{mm}$



c)

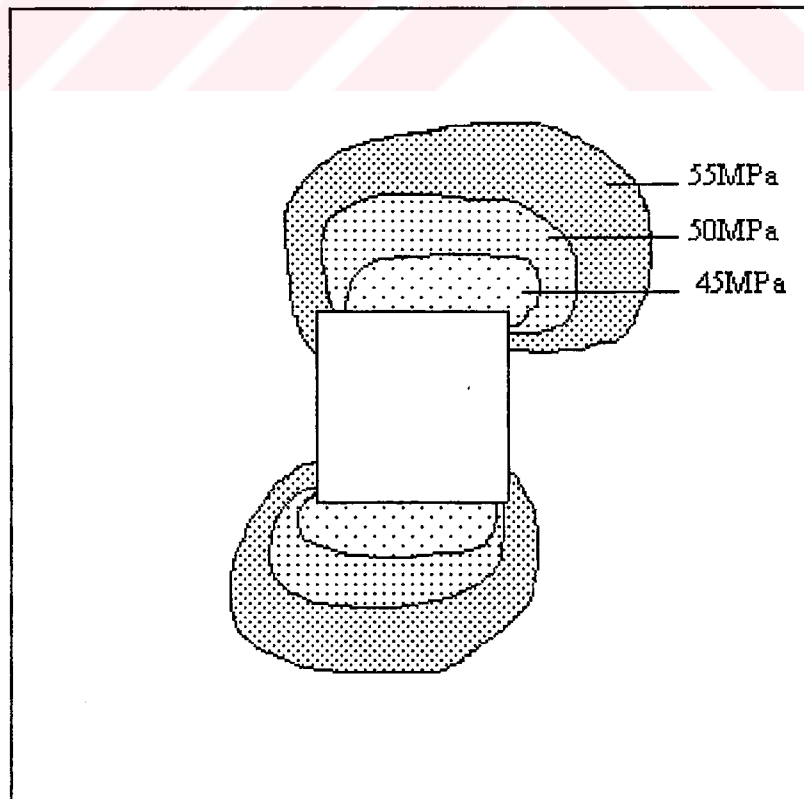
Figure 5. 2 $\theta = 90^\circ$, Plastic regions on quarter plates, a) hole size 20x20mm b) hole size 40x40mm and c) hole size 60x60mm

a= 20mm



a)

a= 40 mm



b)

a= 60mm

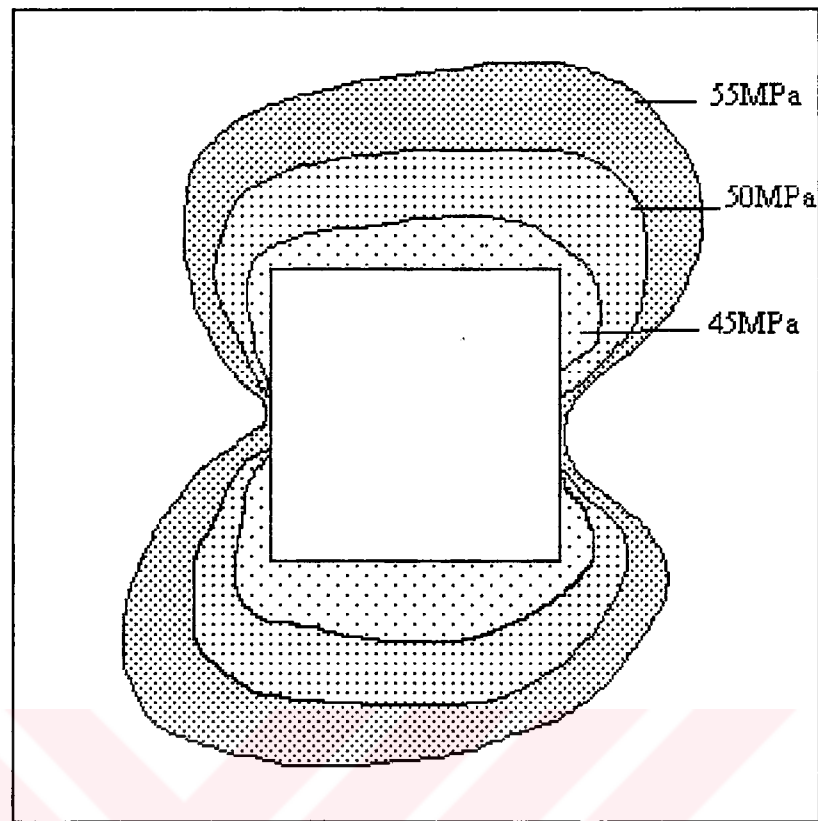
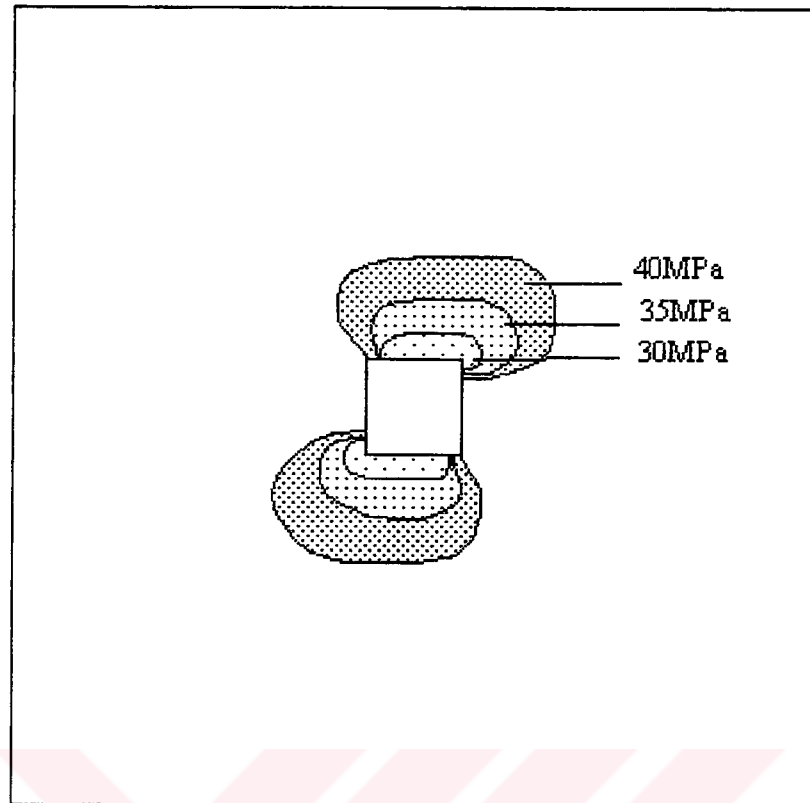
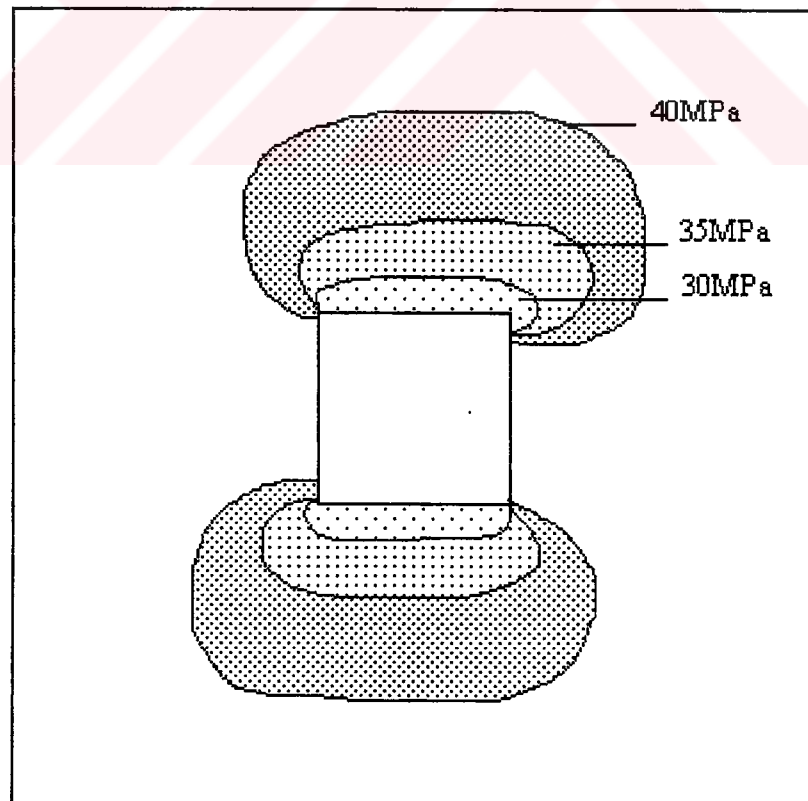


Figure 5.3 $\theta = 30^\circ$, Plastic regions on whole plates, a) hole size 20x20mm b) hole size 40x40mm and c) hole size 60x60mm

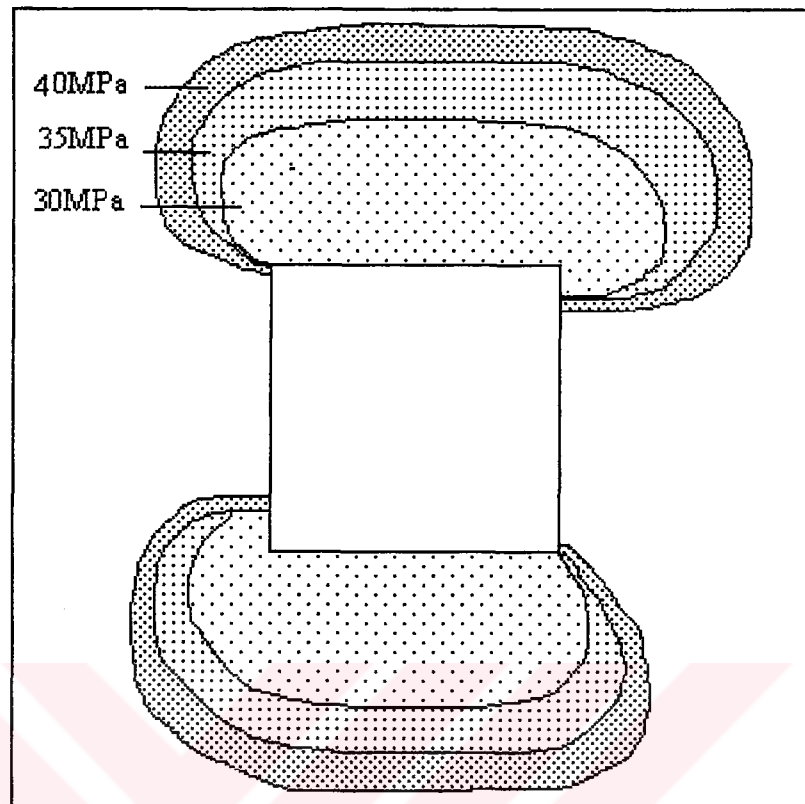
$a=20\text{mm}$ 

a)

 $a=40\text{ mm}$ 

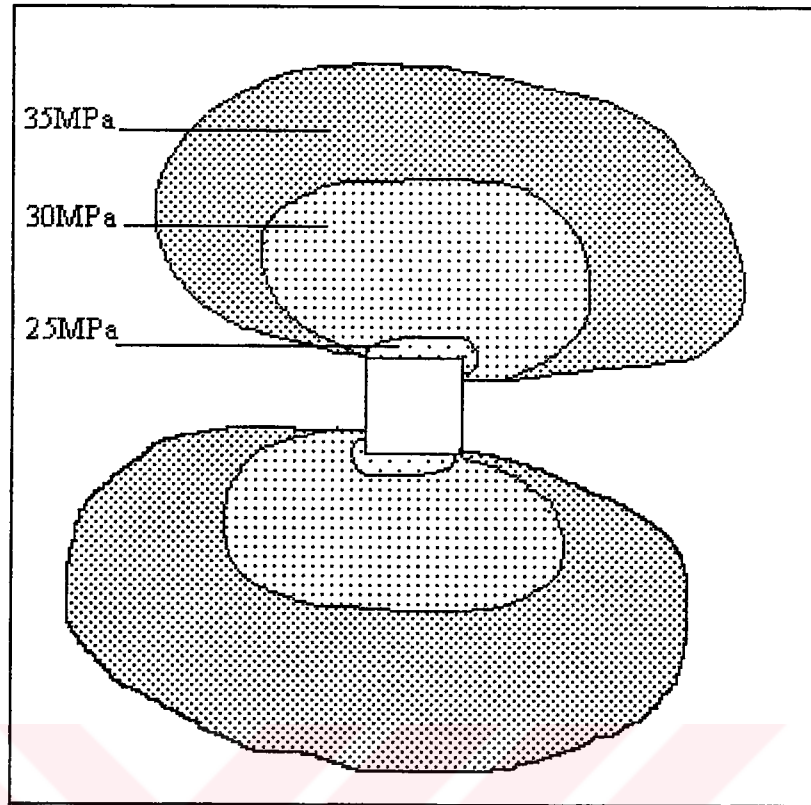
b)

$a=60$ mm

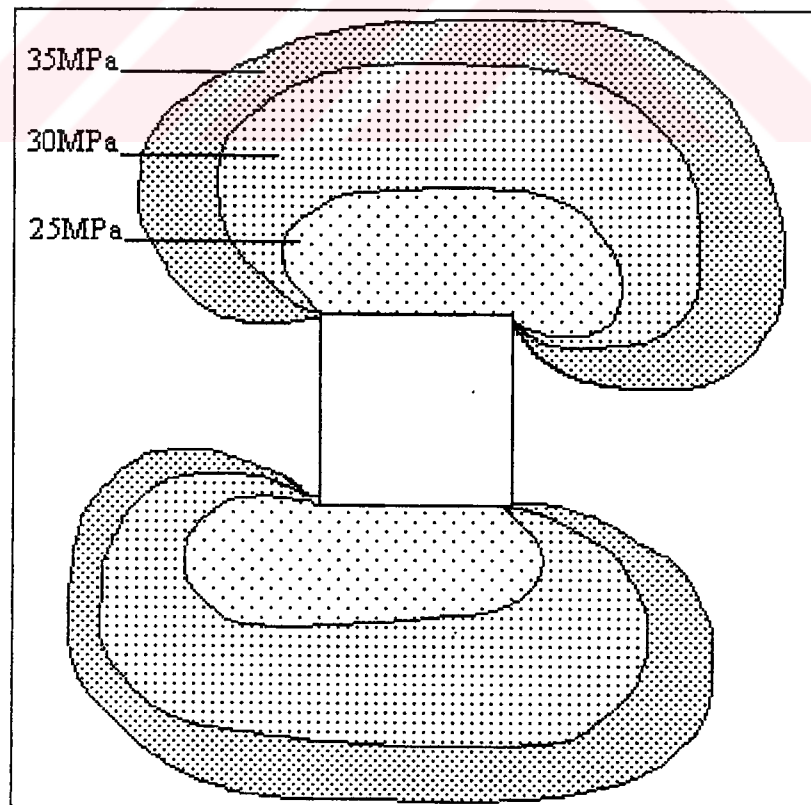


c)

Figure 5. 4 $\theta = 45^\circ$, Plastic regions on whole plates, a) hole size 20x20mm b) hole size 40x40mm and c) hole size 60x60mm

$a=20\text{mm}$ 

a)

 $a=40\text{mm}$ 

b)

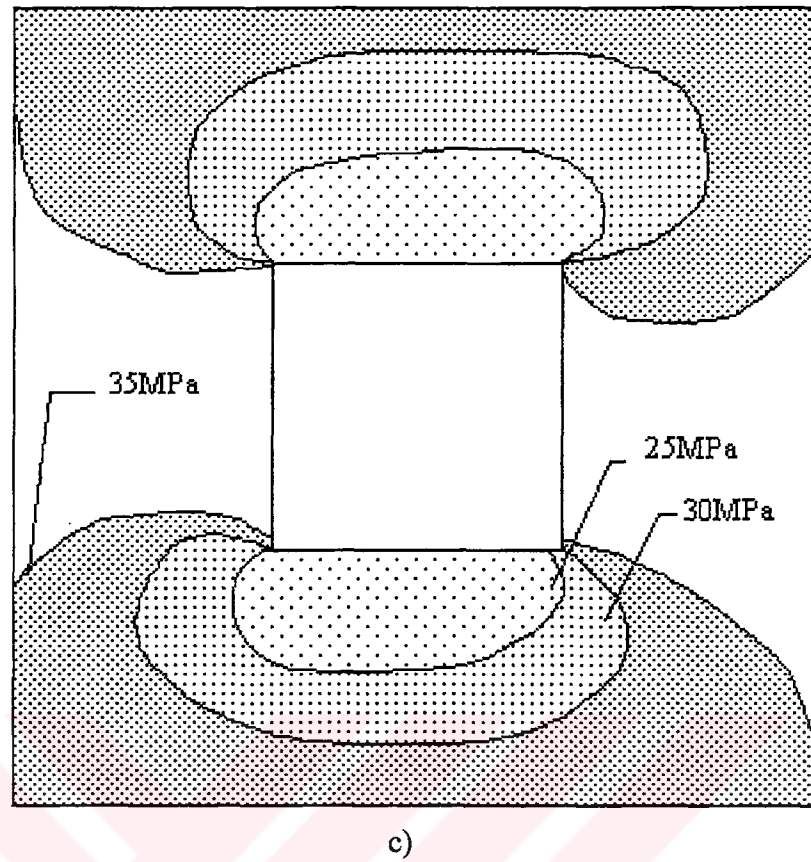
$a=60\text{ mm}$ 

Figure 5. 5 $\theta = 60^\circ$, Plastic regions on whole plates, a) hole size 20x20mm b) hole size 40x40mm and c) hole size 60x60mm

The following figures are shown graphically.

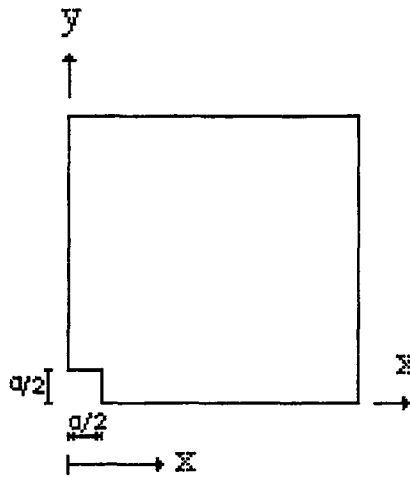
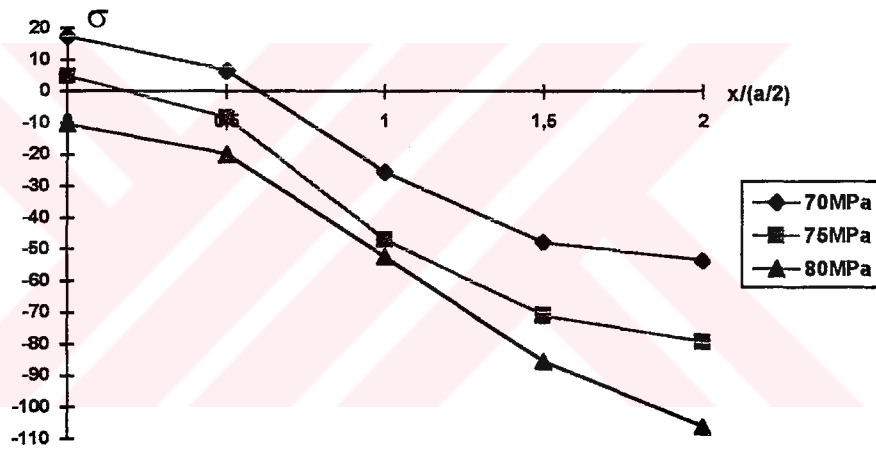
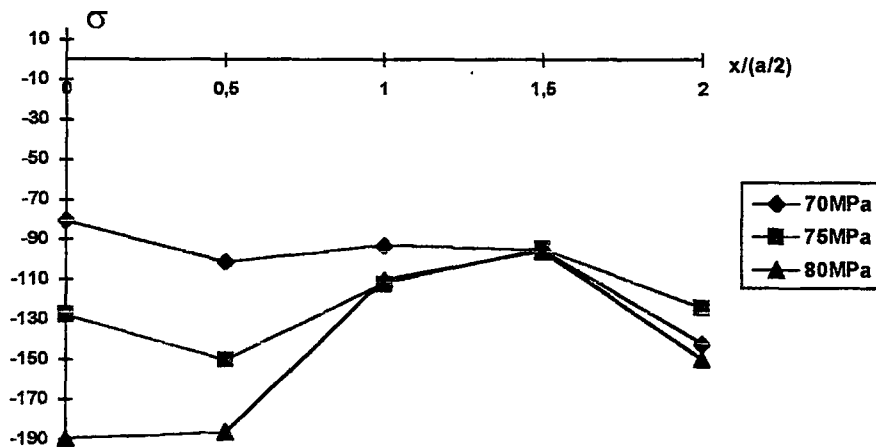


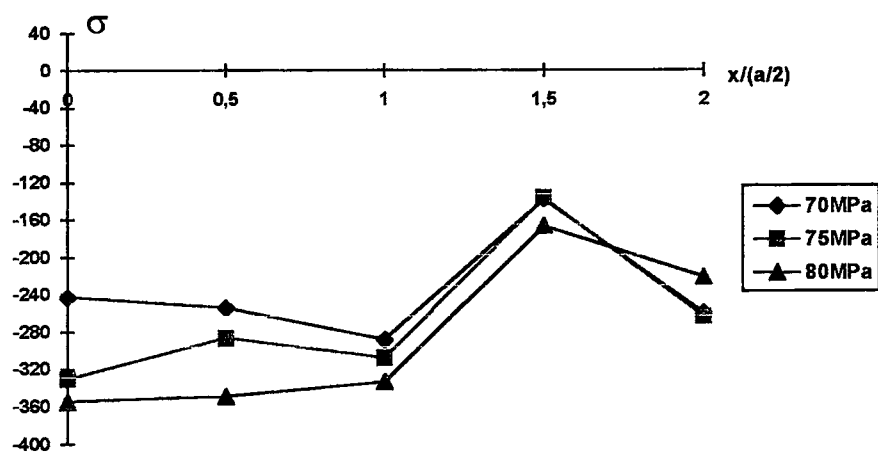
Figure 5. 6 A square plate for graphics



a)

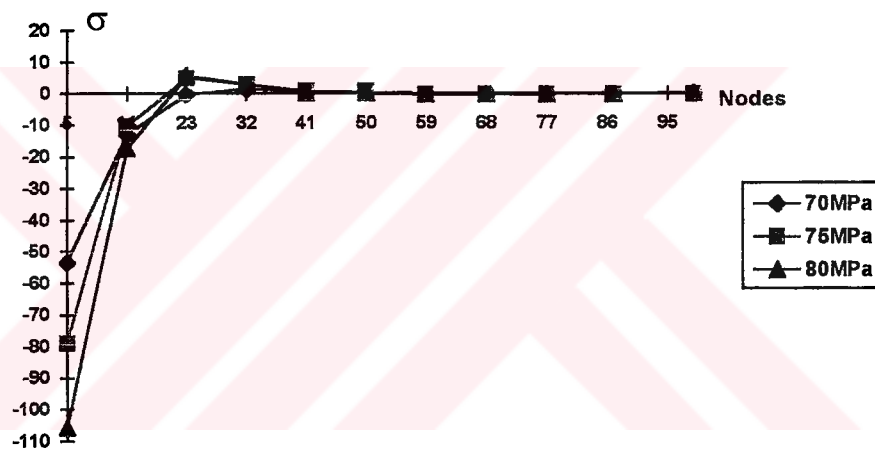


b)

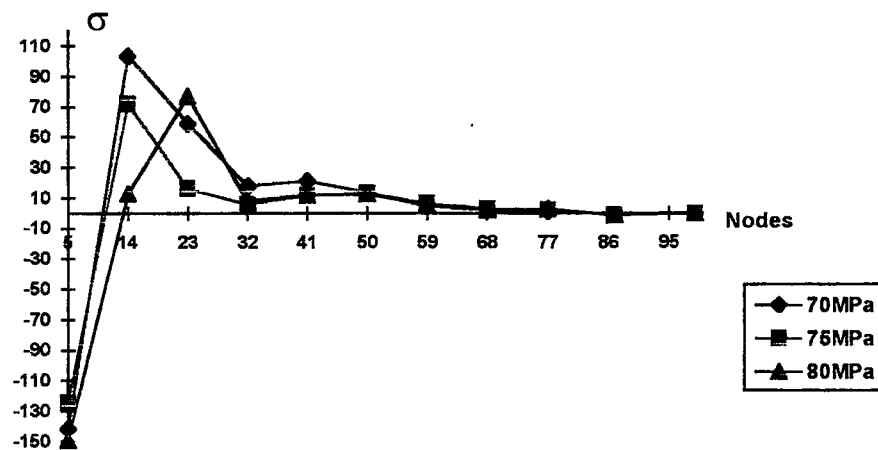


c)

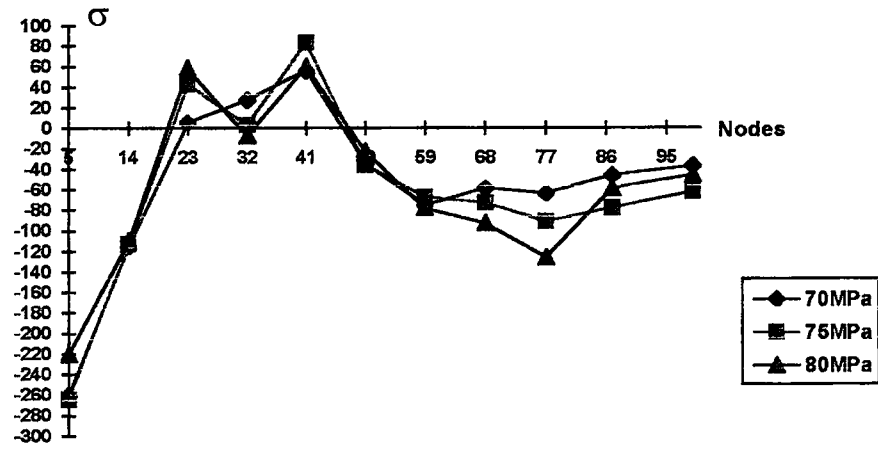
Figure 5.7 $\theta=0^\circ$, Residual stresses (σ) on upper line of the hole, a) hole size 20x20mm, b) hole size 40x40mm, c) hole size 60x60mm.



a)

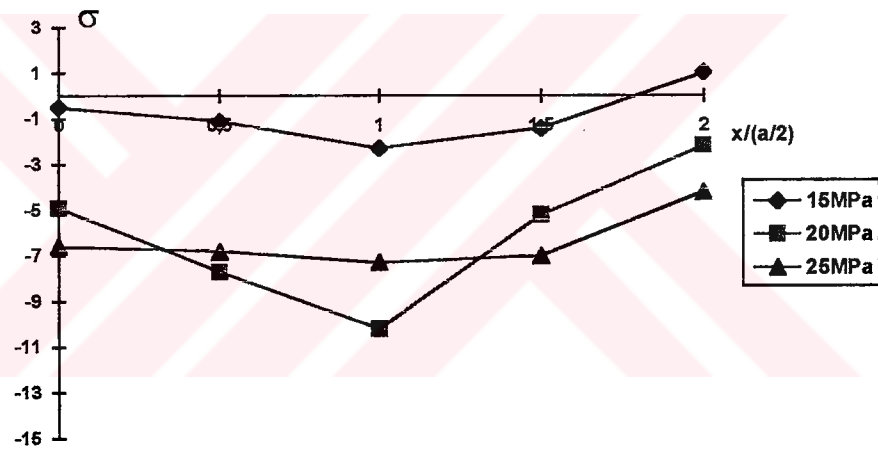


b)

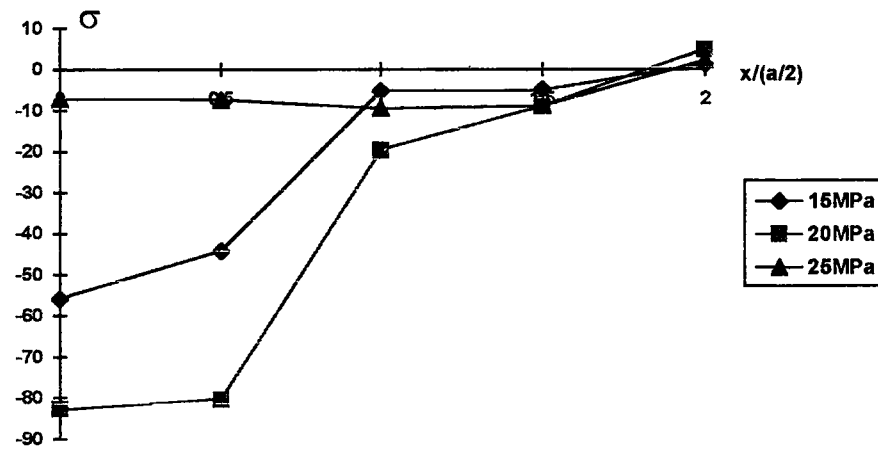


c)

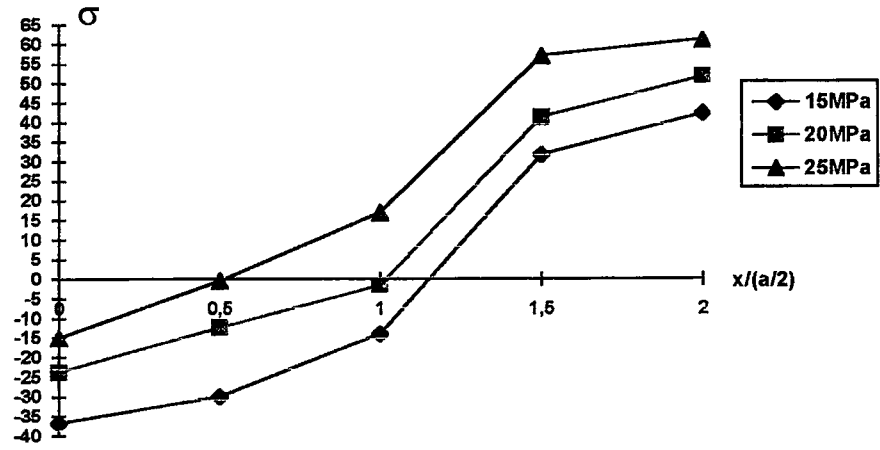
Figure 5. 8 $\theta=0^0$, Residual stresses (σ) on diagonal line
 a) hole size 20x20mm, b) hole size 40x40mm, c) hole size 60x60mm.



a)

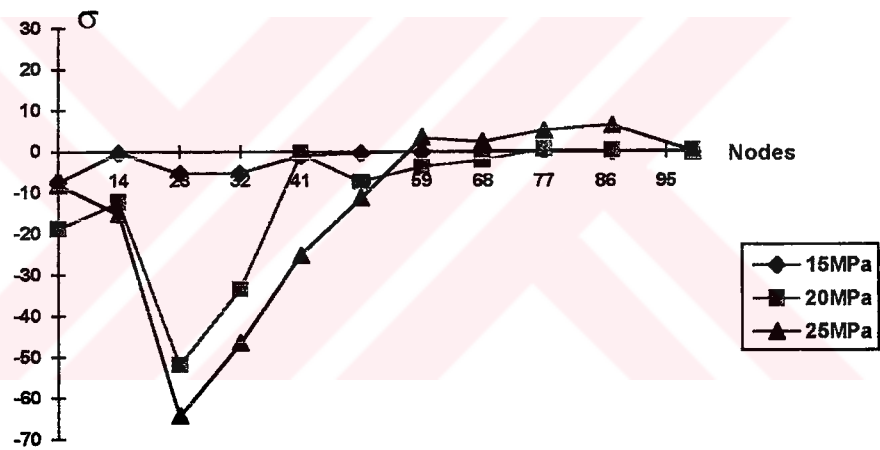


b)

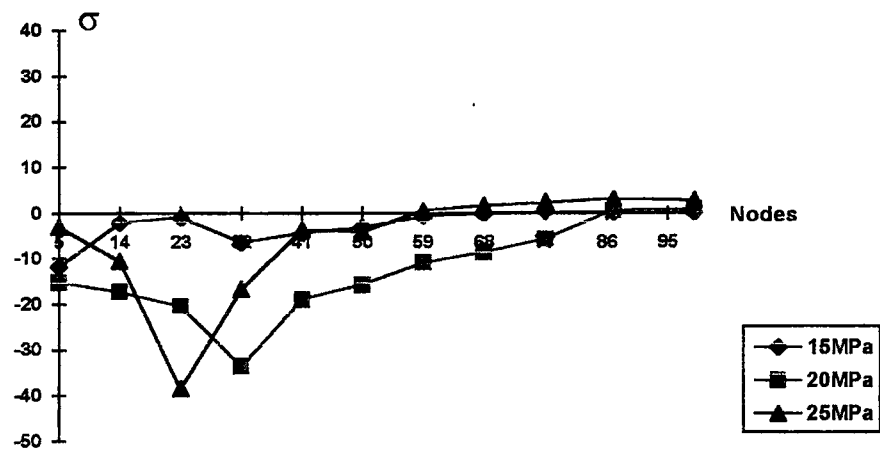


c)

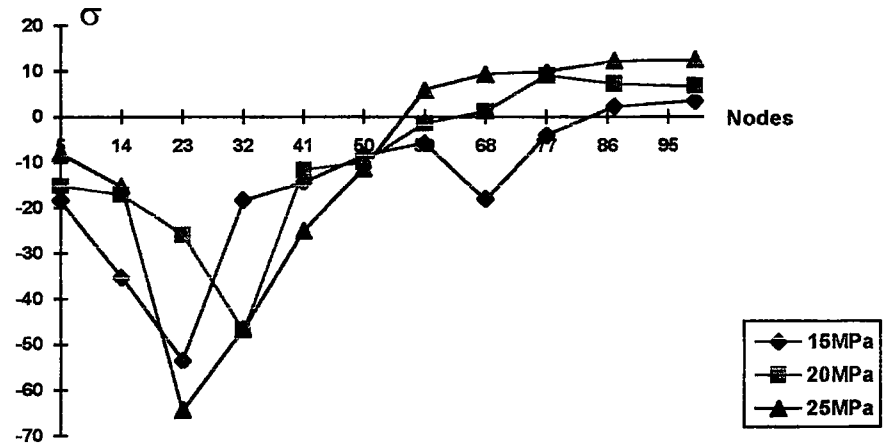
Figure 5.9 $\theta=90^\circ$, Residual stresses (σ) on upper line of the hole,
 a) hole size 20x20mm, b) hole size 40x40mm, c) hole size 60x60mm.



a)



b)



c)

Figure 5. 10 $\theta=90^\circ$, Residual stresses (σ) on diagonal line
 a) hole size 20x20mm, b) hole size 40x40mm, c) hole size 60x60mm.

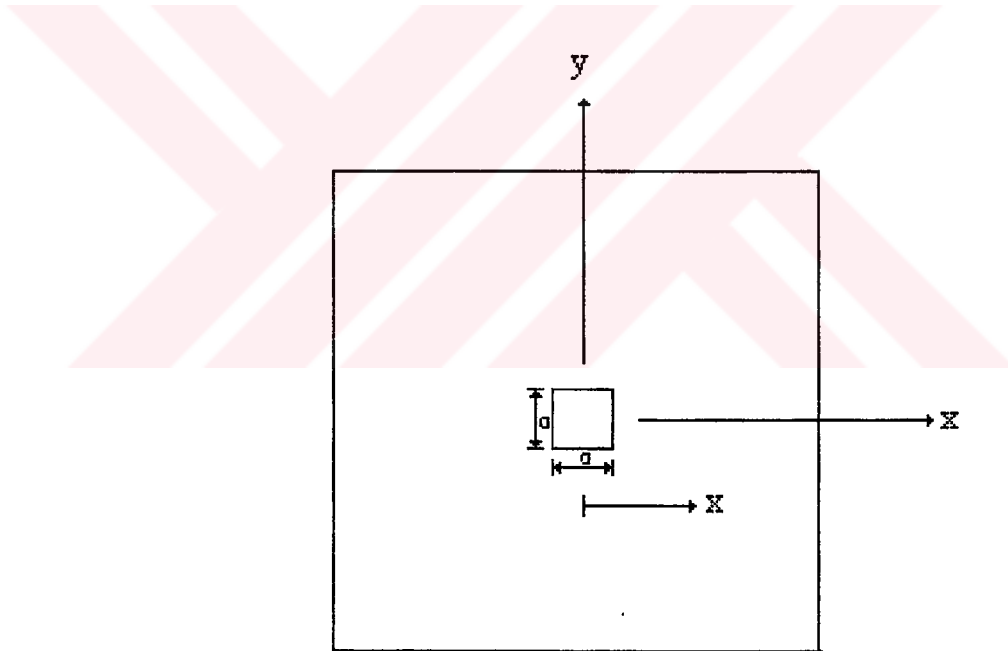
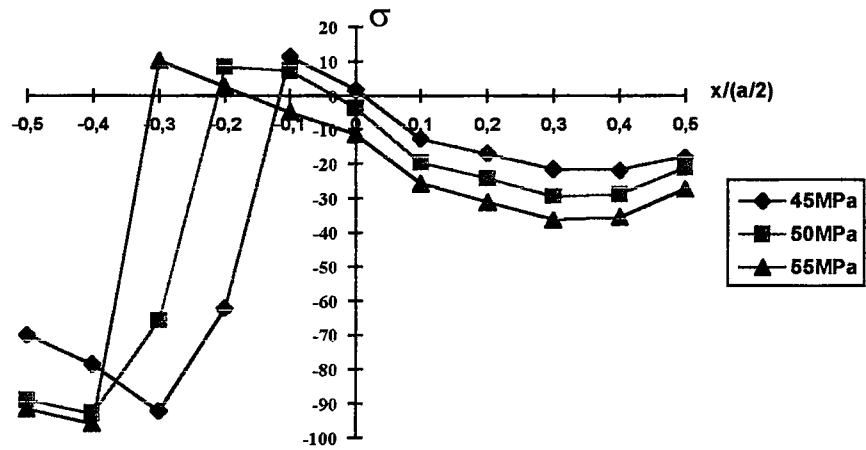
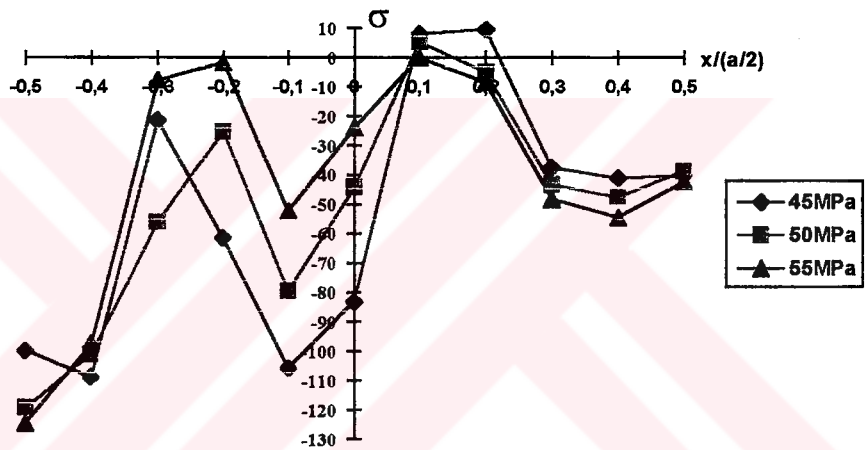


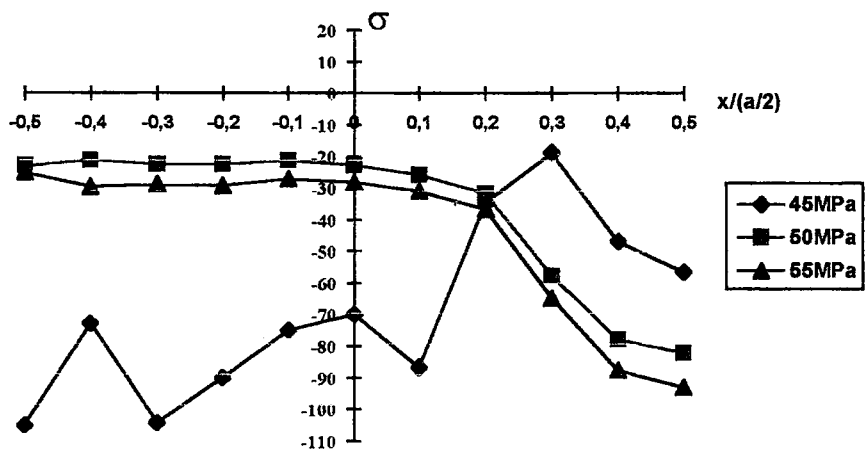
Figure 5. 11 A whole plate for graphics



a)

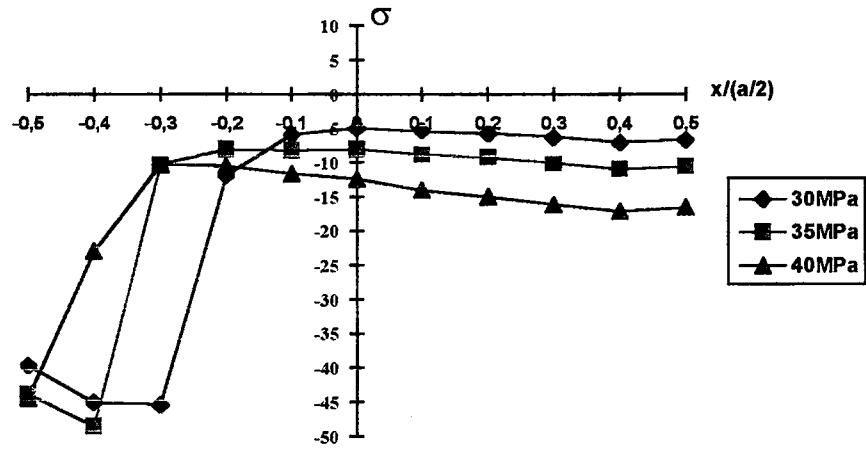


b)

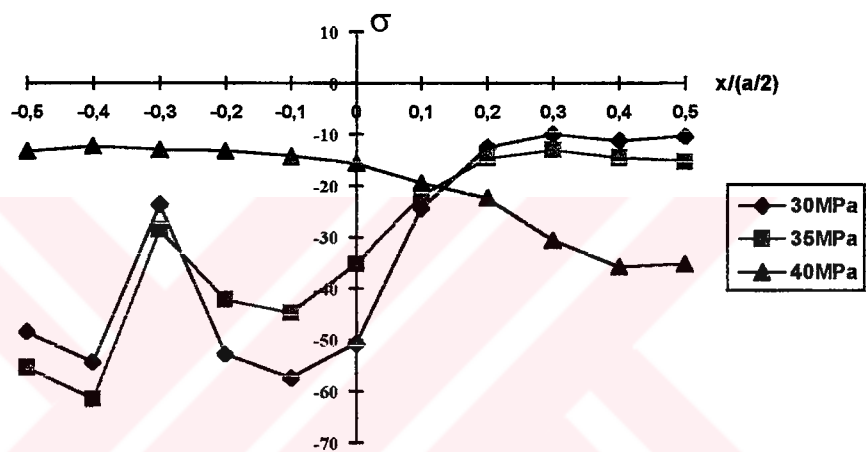


c)

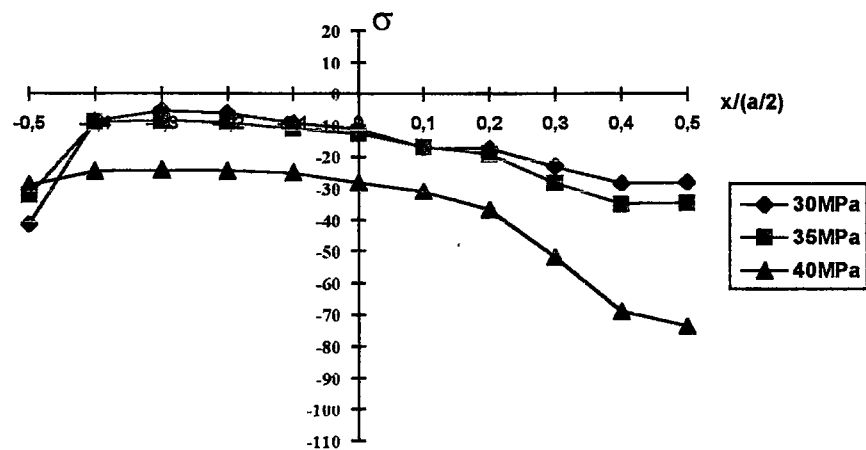
Figure 5. 12 $\theta=30^\circ$, Residual stresses (σ) on upper line of hole
 a) hole size 20x20mm, b) hole size 40x40mm, c) hole size 60x60mm.



a)

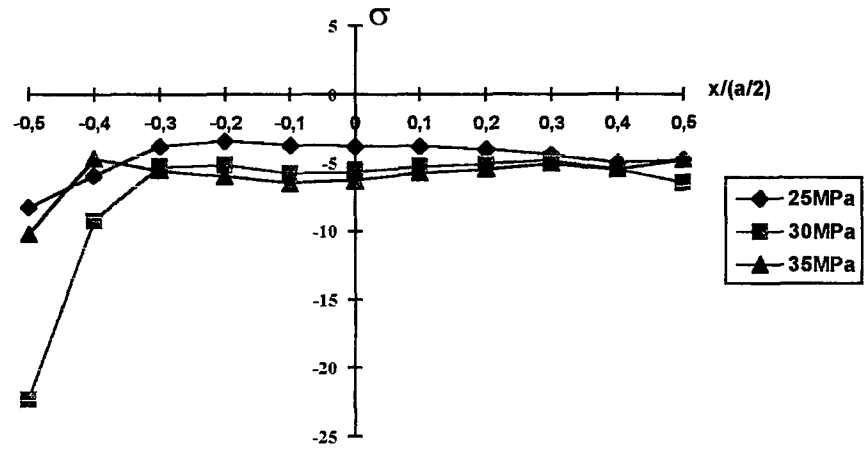


b)

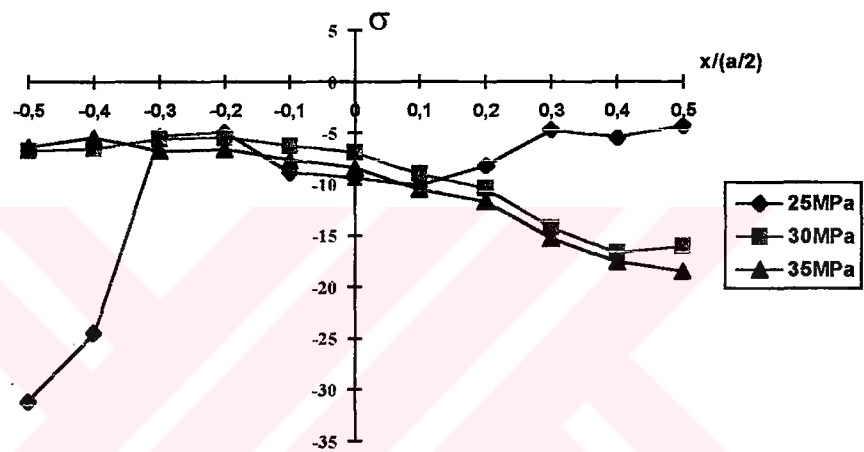


c)

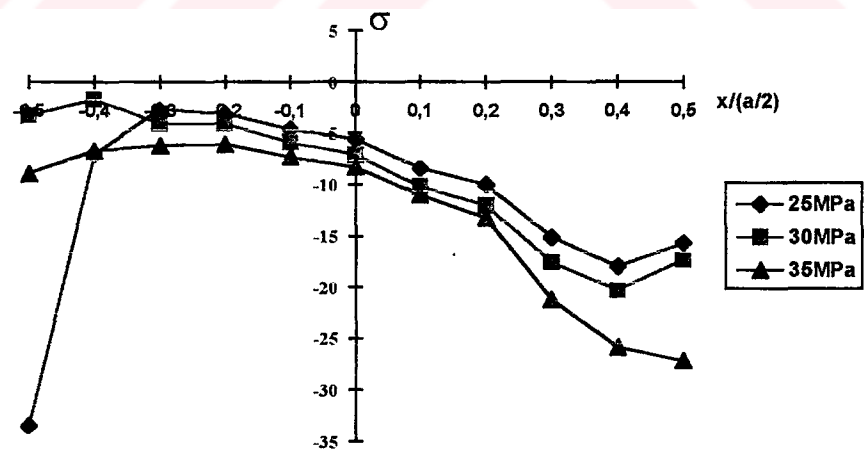
Figure 5. 13 $\theta=45^\circ$, Residual stresses (σ) on upper line of hole
 a) hole size 20x20mm, b) hole size 40x40mm, c) hole size 60x60mm.



a)



b)



c)

Figure 5. 13 $\theta=60^\circ$, Residual stresses (σ) on upper line of hole
 a) hole size 20x20mm, b) hole size 40x40mm, c) hole size 60x60mm.

REFERENCES

1. Jones, R. M., Mechanics of Composite Materials. Dallas, Southern Methodist University, 1975.
2. Karakuzu, R., Orhan, A., Sayman, O., Yarı Dairesel Çentikli Kpompozit Levhaların Elasto-Plastic Zorlamalar Altında Mukavemetinin Artırılması., 5. Ulusal Makina Tasarım ve İmalat Kongresi., pp 449-458. Eylül 1992.
3. Karakuzu, R., Akbulut, H., Sayman, O., Eksenel Yüklü Ankastre Plaklarda Elasto-Plastic Gerilme Analizi, 8. Ulusal mekanik Kongresi., Antalya, pp 361-370, Eylül 1993.
4. Owen, D.R.J. Anisotropic Elasto-Plastic Finite Element Analysis of Thick and Thin Plates and Shells, Int. Journal for Numerical Methods in Eng., Vol.19, pp 541-566, 1983.
5. Sayman, O., Aksoy, S., Kompozit Malzemeler., Ege Üniversitesi, İzmir.
6. Theo de Jong, Stress Around Rectangular Holes in Orthotropic Plates., J. Composite Materials., Vol.15, pp311-328, July 1981.
7. Tirupathi, R., Chandrupatla & Ashok, D., Introduction to Finite Elements in Engineering., Prentice Hall New Jersey., 1991.
8. Tsai, R., Finite Element Stress Analysis of Axisymmetric Bodies Under Torsion., Tecnical Notes., April 1979.
9. Zienkiewicz, O.C., Valliagon, S., King, I.P., Elasto-Plastic Solution of Engineering Problems ' Initial Stress ' Finite Element Approach., Int. Journal for Numerical Methods in Engineering., Vol.1, pp 75-100.